Title
THE FORMATION OF POROSITY DURING DIFFUSION PROCESSES IN METALS

Author
Maher, Dennis M.

Publication Date
1962-09-01

UCRL-10383

University of California

Ernest O. Lawrence Radiation Laboratory

THE FORMATION OF POROSITY DURING DIFFUSION PROCESSES IN METALS

Berkeley, California

DISCLAIMER

UCRL-10383
UC-25 Metals, Ceramics,
and Materials
TID-4500 (19th Ed.)

UNIVERSITY OF CALIFORNIA

Lawrence Radiation Laboratory
Berkeley, California

AEC Contract No. W-7405-eng-48

THE FORMATION OF POROSITY DURING DIFFUSION PROCESSES IN METALS

Dennis M. Maher

(M. S. Thesis)

Metallurgy

September 1962

Printed in USA. Price $1.75. Available from the
Office of Technical Services
U. S. Department of Commerce
Washington 25, D.C.

CONTENTS

THE FORMATION OF POROSITY DURING DIFFUSION PROCESSES IN METALS

Dennis M. Maher

Inorganic Materials Research Division,
Department of Metallurgy
Lawrence Radiation Laboratory
University of California
Berkeley, California

September 1962

ABSTRACT

Evidence is presented which indicates that the porosity formed during diffusion processes in Cu-Ni and Ag-Au couples is heterogeneously nucleated in the presence of a relative excess concentration of vacancies resulting from the unequal mass flow of the two participating constituents. The nature and extent of porosity is dependent on the purity of the sample and thus appears to be related to the number or "potency" of nuclei available for vacancy agglomeration. From metallographic observations on the distribution of porosity, it is estimated that pores will form when vacancies are pumped into any small region of the diffusion zone at the rate of about $10^{15}/cm^3/sec$ in oxygen-free high conductivity copper and $10^{17}/cm^3/sec$ in spectroscopically pure copper. The higher supersaturation required for the nucleation of pores in spectroscopically pure copper is consistent with all the qualitative observations made on the formation of porosity.

Estimates of the relative fraction of the excess vacancies which condense to form pores on the copper-rich side have been obtained in two ways: 1) from the ration of the overall expansion of the couple to the normal Kirkendall shift, and 2) from the ratio of the measured pore volume to that associated with the net vacancy flux, as derived from concentration-

penetration profiles. Both estimates are in reasonable agreement and indicate that upwards of 90% of the excess vacancies agglomerate as pores rather than being annihilated at jogs on dislocations or other sinks; in spectroscopically pure copper, about 50% of the excess vacancies end their lives at pores. It is concluded that, contrary to the usual assumption, dislocations are not very effective sinks for vacancies under conditions (e.g., relatively low vacancy supersaturations) which prevail within the diffusion zone. The observed differences in the extent of porosity in the two grades of copper are believed to be due to differences in nucleating sites available for vacancy condensation rather than to differences in the ease with which dislocation climb can take place in these two materials.

Additional observations indicate that the presence of aluminum oxide particles or clusters in silver has influenced the normal distribution of porosity in silver-gold diffusion couples. These particles or clusters may be acting as favorable sites for vacancy condensation.

I. INTRODUCTION

It is now well established that, in the presence of a chemical activity gradient, the two components of a binary alloy diffuse at different rates.[1,2] This leads to a net mass flow of the constitutents relative to the lattice. This phenomenon – the so-called Kirkendall effect – is manifest by the motion of inert markers which are located within the diffusion zone.[3] If, for example, markers which are assumed to be fixed relative to the lattice are placed at the original weld interface between two dissimilar metals and diffusion is allowed to occur, the interface markers will be displaced toward the side of the couple which is richer in the faster diffusing component, this usually being the side having the lower melting point. The observed marker displacements are considerably greater than can be accounted for by any changes in density due to changes in composition and, significantly, the shifts are proportional to the square root of the diffusion time. Furthermore, in most systems which have been studied, pores of macroscopic size have been observed on the side of the original diffusion interface which originally contained the more mobile constituent.[4-23]

These facts have generally been interpreted as evidence in favor of a vacancy diffusion mechanism in close-packed metals and in alloys of the substitutional type. Thus, a net mass flow of the two constitutents, arising from the presence of a chemical activity gradient, can easily be accounted for on the assumption that vacancies exchange more readily with one component than with the other. The vacancy model implies, therefore, that the net flux of atoms out of the side of the couple containing the more mobile constitutent be counterbalanced by an equivalent net flow of vacancies into this region. The presence of porosity on the side of the couple suffering a net loss of atoms is consistent with the vacancy model since the porosity

may reasonably be supposed to result from an agglomeration of the defect responsible for diffusion.

Since the net flux of vacancies associated with the unequal mass flow of the constitutents is far greater than the concentration of vacancies present in thermal equilibrium, it is necessary to postulate the existence of sources and sinks for vacancies within the diffusion zone. Possible sources and sinks include the external surface of the specimen, grain and subgrain boundaries the dislocations. The available evidence, both experimental and theoretical, indicates that dislocations, by climbing, provide the major sources and sinks for vacancies within the diffusion zone.[1,6,12,14,16,17,22,24-29]

The climb of dislocations implies that plastic deformation must take place during chemical interdiffusion and that deformation processes play an essential role in accommodating the unequal mass flow. The many observations which have been reported on recrystallization,[22,24,26] polygonization,[6,12,16,25,26] grain boundary migration,[24,26] and surface rippling[14,17,22,59,60] within the diffusion zone between dissimilar metals attest to the fact that plastic flow actually does occur and that stresses of appreciable magnitude are generated during diffusion. These various phenomena have been explained in terms of the generation and movement of dislocations by climb or by glide processes.[17,26,59,60]

However, the factors which control or influence the formation of porosity are not nearly so well understood. In particular, only rough estimates are available for the critical degree of vacancy supersaturation required for the nucleation of a pore of stable size, and the details of the nucleation process can only be hinted at in most cases. Seitz[28] has discussed the formation of porosity in the presence of a nonequilibrium

concentration of vacancies and has derived estimates for the critical nucleus size. Brinkman[30] pointed out, however, that these estimates ignored the fact that a two-dimensional tensile stress is established on the side of the interface suffering a net loss of atoms and that, in the presence of this stress, nuclei of a critical size may grow by absorbing vacant lattice sites even when the vacancy concentration is maintained at or near its equilibrium value. This point of view has been debated at length.[31,32] While it is now recognized that mechanical stresses may indeed influence the formation of porosity during diffusion, it appears that, even in the presence of a stress, a critical pore size exists which must be exceeded in order for the nucleus to be stable. This critical size will depend upon the excess vacancy concentration as well as on the magnitude of the stresses within the diffusion zone.

In actual diffusion specimens, the relative excess concentration of vacancies, R_c, required for the formation of a stable pore nucleus, namely,

$$R_c = \frac{N_v}{N_{vo}} - 1,$$

where

N_v = number of vacancies per unit volume actually present in the metal,

N_{vo} = number of vacancies per unit volume in thermal equilibrium,

has been approximated in several ways. For example, calculations of the net flux of vacancies into a given region, based on the observed concentration - distance curves and a knowledge of the intrinsic diffusivities, together with estimates of the sink density have resulted in values ranging from 0.01 to 100 at the position where pores just form in α-brass, the highest value being for zone-refined material.[13,18] Values of R_c of about 0.01 have been estimated for Cu-Ni couples from measurements of the critical pressure required to eliminate pores of known size already formed.[21]

Although these estimates are only approximate, it seems clear that the relative supersaturation at which pores actually form in diffusion specimens is much less than that which would be necessary to nucleate pores homogeneously.[28]

It has therefore been proposed that porosity forms by a process of heterogeneous nucleation[12] and that favored nucleating sites exist either in the bulk of the material or at the original weld interface. Brinkman[30] has argued that stress concentrations which develop within the diffusion zone might nucleate cracks or fissures of a critical size purely by a mechanical means. However, the obvious ease with which such stress concentrations, even if they did arise, would be eliminated by local relaxation and plastic flow makes this possibility appear extremely unlikely.[29] A strong indication that internal surfaces such as particles or inclusions represent effective nuclei for the formation of porosity is provided by the work of Resnick and Seigle.[18] During dezincing experiments on brass of commercial purity they found that porosity developed to a considerable depth below the surface of the specimen after evaporation of only a small amount of zinc. When the brass was zone refined, however, practically no pores were formed within the body of the specimen, even upon complete dezincification. Resnick and Seigle concluded that the most likely nucleating sites in α-brass were zinc oxide particles.

The work to be reported here was undertaken in an attempt to obtain more specific information about the nature of the nucleating sites for porosity in other metals. For this purpose, the formation of porosity and the accompanying dimensional changes were studied in diffusion couples prepared from materials of different purities, as well as materials in which known dispersions of second phase particles were deliberately introduced. The copper-nickel and silver-gold systems were selected for study partly because a complete series of solid solutions are formed in both cases and because

these systems have frequently been investigated in the past. Controlled dispersions of Al_2O_3 particles or clusters were produced in some copper and silver specimens by internal oxidation. Oxide dispersions of this type have the advantage that they are thermodynamically stable at the diffusion temperatures. The average size of the particles is of the order of 500 Å or less in copper[33] and 50 Å or less in silver.[34] It was hoped to obtain estimates for the vacancy supersaturation at which pores are nucleated in these various materials and in this way to assess the relative effectiveness of the Al_2O_3 particles as nucleating sites.

II. EXPERIMENTAL PROCEDURES

Sandwich-type Cu/Ni and Ag/Au diffusion couples with tungsten wire markers embedded at the interfaces were prepared by pressure welding. The nature, distribution, and amount of porosity which develops during diffusion was observed metallographically in couples prepared from components (i.e., Cu and Ag) having different purities. The growth and movement of the zone of porosity was also followed as a function of time using metallographic methods. An attempt was made to correlate the observed porosity with the dimensional changes which normally accompany the diffusion process in sandwich-type couples, and thereby ascertain what fraction of the net vacancy flux is responsible for porosity. For this purpose, interface marker shifts were measured relative to reference markers located well outside the diffusion zone and the fraction of porosity was determined by areal and linear analysis. Concentration-penetration curves were also obtained on a limited number of couples in order to facilitate the above correlation and to permit calculations to be made of the vacancy supersaturation at points where porosity just begins to form within the diffusion zone.

A. Materials

The starting materials employed in this investigation are listed below, along with their nominal purities and the source of supply, where known:

1. Spectroscopically pure copper; 99.999% Cu; American Smelting and Refining Company.
2. Oxygen-free high conductivity copper; 99.99% Cu.
3. Nickel; 99.999% Ni; Mond Nickel Company.
4. Ultrahigh-purity silver; 99.9999% Ag; Consolidated Mining and Smelting Company of Canada, Ltd.

5. Silver; 99.999% Ag; Western Gold and Platinum.

6. Gold; 99.99% Au.

7. Aluminum; 99.999% Al.

The analyses of the spectroscopically pure copper and oxygen-free high conductivity copper (referred to in the remainder of this report as "Spec" copper and "OFHC" copper, respectively) are listed in Table I.

Dilute copper-aluminum and silver-aluminum alloys were prepared from these starting materials; these alloys were then internally oxidized in order to introduce a fine dispersion of second-phase oxide (i.e., Al_2O_3) particles. The copper alloys (nominally 0.10, 0.20, 0.50 at.% Al) were made from a master alloy of OFHC copper - 5 at.% Al. The alloys were melted and cast in an induction furnace under a positive pressure of predried helium. Melting was carried out in an alundum crucible and the alloys were chill cast in a water cooled copper mold. The ingots were machined to eliminate surface defects, and after cold rolling to appropriate thickness, the alloys were homogenized for four days at 990°C in a dynamic vacuum of $\sim 10^{-4}$ mm Hg. In order to accomplish the internal oxidation without the formation of an external cuprous oxide scale, the alloys were embedded in a mixture of cuprous oxide and copper powder and annealed inside a closed iron tube.[35] The 0.10, 0.20, 0.50 at.% Al alloys were internally oxidized at 950°C for 2, 3 and 8 days, respectively. These times were more than adequate to ensure complete oxidation based on the data given by Rhines.[36]

A silver - 0.5 at.% Al alloy was prepared from a master alloy (5.0 at.% Al) by induction melting in a dry helium atmosphere. The alloy was melted in a reactor grade graphite crucible and chill cast into a water cooled copper mold fitted with reactor grade graphite liner. The cast ingot was machined

TABLE I

*Spectrographic Analysis of Spec and OFHC Copper (ppm)

Nominal	Fe	P	C	Sb	Pb	Sn	Ni	Bi	Ag	As	Cr	Si	Te	Se	S	Mn
Spec Cu	<7	-	-	<10	<10	<10	<10	<1	<3	<20	<5	<1	<20	<10**	<10**	-
OFHC Cu	20***	2	<15	<50	<10	<10	<30	<10	<5	<40	-	-	<50	<20***	20**	<10

* Elements listed were not visible spectrographically; values given represent limits of sensitivity of the analytical techniques.

** Chemical analysis

*** X-ray fluorescence analysis

to eliminate surface defects before cold rolling to a thickness of 0.50 cm. The foiled strip was then homogenized at 920°C for 2 days in vacuum. Internal oxidation of the silver alloy was carried out in flowing oxygen at atmospheric pressure. Two bars (18 cm x 1.6 cm x 0.3 cm) milled from the homogenized alloy were supported by a stainless steel wire in the constant temperature zone of a vertical resistance furnace and oxidized for 120 hr at 900°C.

B. Specimen Preparation

For the purposes of these experiments, it was necessary that the component materials be dimensionally stable and also that they be free from any pre-existing porosity. To minimize possible complications from grain boundary diffusion, it was also desirable that a relatively large and stable grain size be established prior to diffusion. Finally, of course, the opposite faces of each specimen had to be as nearly parallel as possible.

It is believed these requirements have been satisfied quite closely. Dimensional stability was achieved by annealing the specimens after final machining for long periods of time in vacuum at temperatures about 50°C higher than the actual diffusion temperatures employed. This treatment also led to the establishment of a stable grain structure, the average grain size in all materials being of the order of several millimeters. The specimens appeared to be completely sound and free from voids or cavities under microscopic examination. Parallelism between the opposite faces of the specimens was maintained by within ± 0.002 cm by careful machining.

Specimens were machined to the form of rectangular parallelepipeds having the following approximate dimensions:

(1) Copper and internally oxidized copper alloys:

2.5 cm x 2.5 cm x 0.3 cm.

(2) Nickel: 2.5 cm x 2.5 cm x 0.2 cm.

(3) Silver and internally oxidized silver alloys:
1.6 cm x 1.6 cm x 0.3 cm.

(4) Gold: 1.6 cm x 1.6 cm x 0.04 cm.

The large surfaces of each sample were carefully ground by hand through No. 4/0 emery paper after machining and final heat treatment. Extreme care was taken to ensure that the ground faces remained plane parallel. After grinding on the papers, the specimens were polished on a vibratory polishing wheel using 3μ diamond paste on a silk cloth. In this manner specimen flatness was maintained and the resulting surfaces were smooth on a microscopic scale. Immediately prior to assembling a diffusion couple, the polished surfaces were given two or three light passes on No. 4/0 emery paper in order to roughen them so as to increase the point contact at each interface. Finally, the samples were washed with soap and water, rinsed first in acetone and then absolute alcohol, and dried between filter papers.

C. Assembly and Welding of Diffusion Couples

Each diffusion couple consisted of six individual pieces, assembled as shown in Fig. 1. In all couples interface "0" represents the reference plane relative to which the marker shifts were measured. Table II lists the various couples which have been examined in this study.

A special jig was designed which greatly facilitated accurate positioning of the markers (1 mil tungsten wire) at the respective interfaces before welding. In the Cu-Ni couples, 15 parallel wires spaced approximately 1.5 mm apart were placed at each interface; 10 parallel markers, also spaced about 1.5 mm apart, were inserted at each interface in the Ag-Au couples.

The constituent pieces were inserted in a stainless steel clamp which was securely tightened. A thin coating of alumina was first applied to the

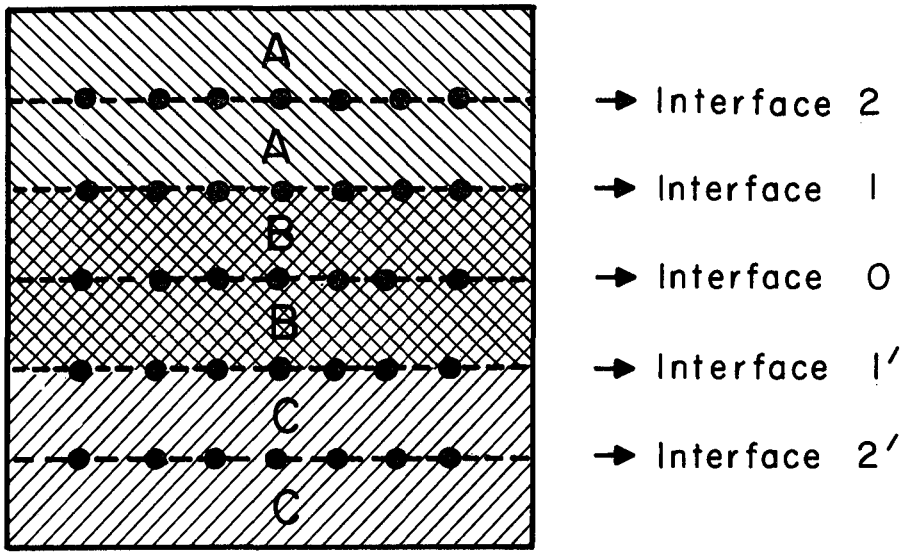

Fig. 1. Assembled diffusion couple of the A/B/C type. The various marker interfaces are distinguished by number.

TABLE II

Diffusion Couples Examined in this Investigation

Number	Type of Couple: A/B/C
1	Spec Cu/Ni/OFHC Cu
2	Spec Cu/Ni/Cu-Al-O (0.1 At. % Al)
3	Spec Cu/Ni/Cu-Al-O (0.2 At. % Al)
4	Spec Cu/Ni/Cu-Al-O (0.5 At. % Al)
5	Ag (99.999%)/Au/Ag (99.9999%)
6	Ag (99.999%)/Au/Ag-Al-O (0.5 At. % Al)

stainless steel end plates in order to prevent the specimens from bonding to the clamp during the welding operation. Pressures of approximately 2000 psi (Cu-Ni system) and 1000 psi (Ag-Au system) were applied to the faces of the clamp so as to embed the markers and to bring the specimen surfaces into intimate contact. After tightening, the entire assembly was heated in vacuum in order to pressure weld the individual sections of the couple together. Initially, an OFHC Cu/Ni/OFHC Cu couple and a Ag/Au/Ag couple were satisfactorily welded without markers merely by heating under pressure for 1 hr at 750°C in vacuum (10^{-3} - 10^{-4} mm Hg) and then allowing the assembly to cool slowly in the furnace. Metallographic examination indicated that all of the weld interfaces had remained plane and that they were free from voids or cavities.

A slightly more refined technique was employed in welding couples containing markers. The welding operation was carried out in an all metal high vacuum furnace capable of reaching pressures as low as 10^{-8} mm Hg. A Spec Cu/Ni/OFHC Cu couple of the type shown in Fig. 1 with markers placed

at each of the interfaces was welded soundly using the following procedure:

1. The furnace was evacuated to about 10^{-7} mm of Hg.
2. The temperature was raised to 800°C and stabilized while the clamp containing the sample was supported in the upper (cold) portion of the vertical resistance furnace.
3. The assembly was slowly lowered into the hot zone and held for approximately 1 hr at 800°C at a pressure of approximately 10^{-6} mm Hg, after which it was raised back up into the cold zone and allowed to cool to room temperature.

In view of this early success, no difficulty was anticipated welding couples having an internally oxidized alloy as one of the components. As it turned out, however, the same procedure as that described above failed to yield acceptable welds with Cu-Ni couples of type 2,3, and 4. Metallographic examination following preliminary (25 hr) diffusion anneals at 900°C showed that the three similar interfaces (2, 0, and 2') and the high-purity copper-nickel interfaces (1) were sound, but that the Ni/Cu-Al-O interfaces (1') had not been adequately welded.

Consequently, the welding conditions, i.e., time, temperature, and pressure, were varied over wide limits in an attempt to overcome this problem. Despite exhaustive efforts, however, a satisfactory method of welding has not yet been found. There appeared to be a number of possible reasons for the failure to weld the internally oxidized copper to nickel. For example, the presence of a thin oxide film on the surface of the components might have prevented adequate diffusion from taking place. These oxide films would probably not have been broken down mechanically as a result of plastic flow at the interfaces, nor would they have "dissolved" during welding since the copper was already saturated with oxygen.

It could not be established with certainty by metallographic examination alone whether or not sound welds had been obtained at each of the various interfaces. In fact, it was generally necessary to carry out at least a preliminary diffusion anneal (25 hr at 900°C for Cu/Ni couples; 1 hr at 875°C for Ag/Au couples) in order to ascertain the quality or character of the weld interfaces. Couples which were poorly welded sometimes fell apart immediately following this preliminary anneal (or during subsequent anneals). In a few cases, the presence of voids or cavities due to faulty welding could be recognized and distinguished from the porosity resulting from diffusion. In general, however, the soundness of the dissimilar interfaces (1 and 1') was difficult to assess even after the initial diffusion anneals, except by carrying out some type of destructive test. Consequently, all couples which appeared to be welded, judging from the appearance of the interfaces under the microscope, and which remained intact after the preliminary diffusion treatment, were carried through subsequent diffusion anneals.

D. Diffusion Anneals

The diffusion anneals were carried out in a closed quartz tube under a positive pressure of high purity argon. The quartz container was initially evacuated to about 5×10^{-7} mm Hg, flushed with argon, re-evacuated, and filled with argon to a pressure of approximately 1/4-atmosphere. The sandwich-type couples were supported inside the tube on two high-purity alumina knife edges. The quartz tube was inserted in a vertical resistance furnace after the desired temperature in the hot zone had been established and stabilized. After a predetermined diffusion time, the tube containing the specimen was withdrawn from the furnace and allowed to cool to room temperature. Because of the relatively rapid heating and cooling rates, no corrections were

necessary for the amount of diffusion which occurred during heating and cooling.

All diffusion anneals in the Cu-Ni system were carried out at 900°C; the Ag/Au couples were all diffused at 875°C. A close check on temperature conditions in the hot zone was made throughout the diffusion anneal using a calibrated platinum-platinum rhodium thermocouple. Temperature fluctuations during a run were with ±1°C. It is believed that the actual temperature of the sample was known to with ±3°C.

E. Metallographic Observations on Nature, Distribution, and Amount of Porosity

The nature, distribution, and amount of porosity which normally accompanies the diffusion process was evaluated metallographically. In addition, the surface topography of the couples in the vicinity of the diffusion zone was studied. After each diffusion treatment, the couple was carefully polished in a plane perpendicular to the weld interface and photomicrographs were taken to illustrate the distribution of porosity and the effect of interface markers on this distribution.

The metallographic preparation of couples required extreme care in order to obtain a true indication of the nature and extent of the porosity. Conventional practices were, in general, inadequate, especially for the Ag-Au couples, in which a large number of interconnected pores form very early in the diffusion process. Vibratory polishing techniques[37] using fine diamond abrasives, followed by hand polishing on a silk cloth with 1/4 μ-alumina (Linde A) slurry resulted in a reasonably satisfactory polish with Cu-Ni couples. The Ag-Au couples had to be polished entirely by hand to prevent excessive smearing and enlarging of existing cavities. A variety of polishing cloths ("Metcloth", nylon, silk, and "Microcloth") and abrasives were

tried during the rough polishing period. The alumina slurry on a nylon cloth generally gave the most satisfactory final polish.

The fraction of porosity was determined by areal analysis. This was done by superimposing a square grid on the projection screen of a Leitz metallograph and counting the fraction of grid intersection points (out of a total of 840) occupied by pores. The entire interface was sampled in a random fashion.

With the Cu-Ni couples, an electrolytic etching technique first suggested by Barnes[38] was used in order to determine the distribution of porosity with respect to grain boundaries and to locate the position of the etch limit on the nickel side of the couple. The electrolyte consisted of one part concentrated nitric acid and two parts methyl alcohol; a current density of 1.5 amp/cm^2 was employed, the etching time being 3 to 5 sec. In addition, the position of the etch limit with respect to the reference interface, "0", was measured with a traveling microscope.

F. Measurement of Dimensional Changes and Motion of Porous Zone

The distances between marker interfaces were determined with a traveling microscope having an accuracy of ±0.5 μ; the measurements were reproducible to within ±2 μ and were always made with respect to the center of the wire marker itself. The couple was placed in a suitable holder which was attached directly to the movable stage of the microscope. This holder was designed so as to allow both a rotational adjustment with respect to the direction of travel and a tilt adjustment with respect to the direction of incidence of the light source. Hence, it was always possible to ensure that measurements were made in a direction perpendicular to the reference interface and that the plane of the sample was perpendicular to the optic axis of the microscope.

Before and after each diffusion anneal, the surface was carefully polished metallographically and the distance between individual markers was measured. The marker displacement Δ was calculated from

$$\Delta = x_t - x_o \tag{1}$$

where

x_o = initial distance between a reference marker, located well outside the diffusion zone, and a moving marker,

x_t = the distance between the same two markers after a diffusion time t.

It was assumed that the markers at interface "0" were fixed relative to the lattice as well as to a reference point outside the specimen and that the markers at the interfaces 1, 1', 2, and 2' had been displaced as a result of the unequal mass flow during diffusion. In view of this assumption, the following generalized notation was adopted in regard to the marker shifts:

$$\Delta_1 = (x_t)_{10} - (x_o)_{10} \tag{2}$$

$$\Delta_2 = (x_t)_{20} - (x_o)_{20} \tag{3}$$

$$\Delta_3 = \Delta_2 - \Delta_1 = (x_t)_{20} - (x_t)_{10} \tag{4}$$

where

Δ_1 = the displacement of the marker at interface "1" with respect to a reference marker at interface "0" on the B side. This is usually called the "Kirkendall shift."

Δ_2 = the displacement of the reference marker at interface "2" on the A side with respect to a reference marker at interface "0" on the B side. This represents the overall expansion of the couple.

Δ_3 = the displacement of the marker at interface "1" with respect to a reference marker at interface "2" on the A side.

This notation is illustrated schematically in Fig. 2a. The corresponding shifts which occur at interfaces 1' and 2' are designated by Δ_1', Δ_2', and Δ_3', respectively. It is evident from Eq. (4) that only two of these marker shifts, namely Δ_1 and Δ_2 (or Δ_1' and Δ_2') have been measured independently.

The motion of the porous zone with time was followed in a manner similar to the marker displacements, i.e., interface "0" was assumed to be fixed and hence taken as the reference position. Therefore,

$$\Delta_I = (x_t)_{I\,0} - (x_o)_{10} \tag{5}$$

$$\Delta_{II} = (x_t)_{II\,0} - (x_o)_{10} \tag{6}$$

$$W = \Delta_{II} - \Delta_I = (x_t)_{II\,0} - (x_t)_{I\,0} \tag{7}$$

where

Δ_I = the displacement of the boundary (I) of the porous zone closest to the interface marker after time t,

Δ_{II} = the displacement of the outermost boundary (II) of the porous zone after time t,

W = the width of the porous zone after time t.

This notation is represented schematically in Fig. 2b.

G. Concentration-Penetration Curves

Concentration-penetration curves were obtained on a Spec Cu/Ni/OFHC Cu couple after 720 h of diffusion at 900°C. A production model XR 710 -- Applied Research Laboratories electron probe microanalyzer was used for this purpose. The unit was operated at 25 kv with an effective probe diameter of 2-3 μ and probe current of approximately 0.57 μ-amp; measurements

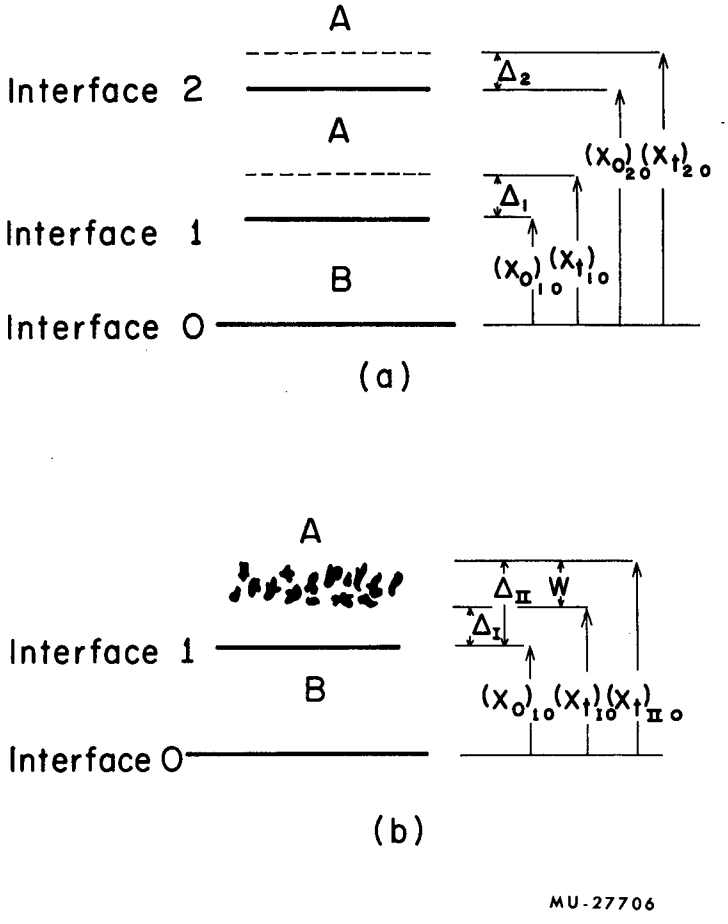

Fig. 2. Notation used in evaluating (a) dimensional changes, and (b) motion and width of the porous zone from the experimental measurements.

were made only under stable probe conditions. The electron beam was incident at 90° to the surface and the X-ray take off angle was 52 $\frac{1}{2}$ °.

A step scan analysis was performed between the two markers whose average displacements, $\bar{\Delta}_1$ (or $\bar{\Delta}_{1'}$), came closest to the average of the entire set of 15 markers. Between each measurement, the specimen was moved a predetermined distance of anywhere from 5 to 100 μ in the direction of diffusion. The integrated intensities of the CuKα and NiKα radiation emitted from the sample were monitored simultaneously. The observed X-ray emission intensities for copper and nickel were converted to percent composition by using the measured intensities of the pure materials as standards and following the correction procedures recommended by Birks[39] (see Appendix).

In addition, profiles were obtained along a line parallel to the diffusion direction at the markers which exhibited the minimum and maximum Kirkendall shifts (Δ_1 or $\Delta_{1'}$). The profiles obtained in this case consist of an instantaneous chart recording of the X-ray intensity, the chart position being coordinated with the movement of the specimen stage; one element at a time was monitored and stage movements of 96 μ per min were employed.

Concentration profiles were also obtained parallel to the Cu-Ni weld interface i.e., normal to the diffusion direction, in the vicinity of the two markers between which the step scan analysis was taken. These measurements were made on the copper side of the couple at distances of 100 and 200 μ from the weld interface.

III. RESULTS

In the Cu-Ni system, marked differences in the amount and distribution of porosity and in the dimensional changes accompanying diffusion have been observed between couples prepared from Spec Cu and OFHC Cu. A detailed study of the porosity and marker shifts has been made in both couples and the results obtained are reported and compared below. The difficulty experienced in welding the internally oxidized copper alloys precluded a similar investigation with these materials. Welding problems were also encountered in the Ag-Au system although this did not become apparent in some cases until the couples had been diffused for times as long as 50 hours. Since the soundness of the original Ag-Au weld interface was in question even in those couples which remained intact, only a limited number of qualitative observations will be reported for this system.

A. Nature, Distribution and Amount of Porosity

1. Cu-Ni System

In agreement with the results of previous studies[5,7,9,10,12-14] metallographic examination disclosed a progressive increase in the amount of porosity formed on the copper side with increasing diffusion time. A significant difference in the extent and distribution of the porosity was observed, however, between Spec Cu and OFHC Cu. This is illustrated in Fig. 3 in which the distribution of porosity in the two grades of copper is compared after 480 h and after 720 h of diffusion at 900°C. It is evident that after equivalent diffusion times, the porosity is distributed over a much wider band parallel to the weld interface in the OFHC Cu/Ni than in the Spec Cu/Ni couple. In both systems, the total number of voids within the porous zone was found to increase with time, this increase being

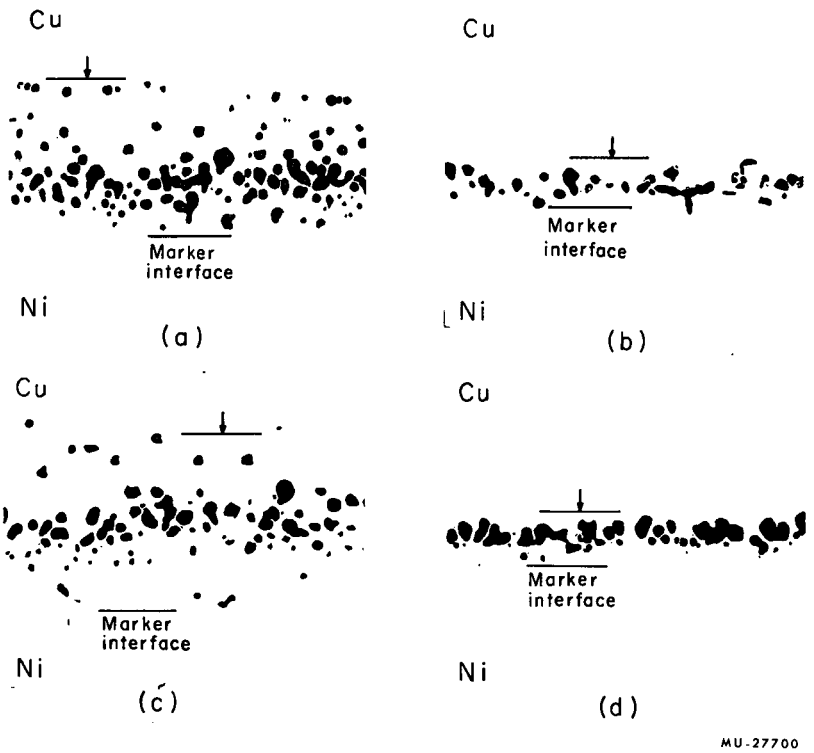

Fig. 3. Comparison of porosity developed in OFHC copper/nickel and Spec copper/nickel couples diffused at 900°C. Arrow indicates limit of porous region. Unetched; 55X. (a) OFHC copper/nickel, 480 h; (b) Spec copper/nickel, 480 h; (c) OFHC copper/nickel, 720 h; (d) Spec copper/nickel, 720 h.

more apparent between 240 and 480 hours than during the next 240 hours. Most striking, however, was the marked increase in the width of the porous zone with time in OFHC copper; in addition, voids in OFHC Cu were frequently observed relatively far in advance (i.e., further toward the pure copper side) of the main body of the porous zone. In contrast, there was only a moderate growth in width of the porous zone with time in the Spec Cu/Ni couple and individual pores were seldom seen at any appreciable distance beyond the rather sharply defined boundary of the porous region.

After 240 h the majority of pores appeared to be completely isolated in both OFHC copper and Spec copper. In general, this was still true in OFHC Cu/Ni after longer diffusion times. On the other hand, the growth of individual pores in Spec Cu/Ni was great enough after 720 h so that, in many cases, the pores now appear to be interconnected (see Fig. 3d).

A significant number of pores were found to have crystallographic outlines, especially after diffusion for 720 h. In fact, pores within a given grain frequently exhibited straight sides with common directions. Three-, four-, and six-sided shapes have been observed. Crystallographic characteristics are expected since, given sufficient time, the bounding surfaces of the pore would tend to assume a minimum energy configuration with certain low index planes being preferred. Barnes,[6] investigating porosity in Cu/Ni couples, reported that many of the straight sides of pores were parallel to slip lines within the same grain, suggesting that the pore faces are parallel to {111} planes.

In the as-welding condition, the tungsten wires were soundly embedded at each interface, and no voids were observed around any of the markers. After diffusion, however, voids developed at the markers on the copper-rich side, and these grew to substantial size with increasing time. This

effect was somewhat more pronounced in Spec Cu/Ni. In some instances, the void which partially surrounded the marker actually appeared to migrate away, leaving the marker in a relatively sound environment. When this happened, the void, after its displacement, still retained the curved shape of the wire marker around which it had originally formed. The observations indicate that the tungsten marker itself is an effective sink for vacancies. As such, the markers also have a noticeable effect on the distribution of porosity, especially in Spec Cu.

This can be seen from Fig. 4 in which the nature of the porosity in the vicinity of the interface markers is shown after 720 h of diffusion at 900°C. In OFHC Cu (Fig. 4a) the width of the porous band is only slightly perturbed at each marker, and pores are formed immediately in advance of the markers on the copper-rich side. In Spec Cu, however, the distribution of porosity is so strongly influenced by the markers (Fig. 4b) that the porous band assumes a sinusoidal form; moreover, porosity is completely absent in the region immediately in advance of the marker. This again suggests that the marker is acting as an effective sink.

Seith and Ludwig[14] previously reported that the number of pores which were formed in a copper-nickel couple was somewhat smaller in the immediate vicinity of tungsten markers (~ 20 μ). The more recent observations by Meechan and Lehman[40] concerning the formation of porosity in "pure" copper in the presence of a large temperature gradient are also pertinent. They found that the porosity developed along a curved trace which dipped down to the quartz fibers (~ 25 μ) that were used as interface markers, leaving a pore free region immediately above the markers. In many respects the porosity observed in Spec Cu is similar to that seen by Meechan and Lehman.

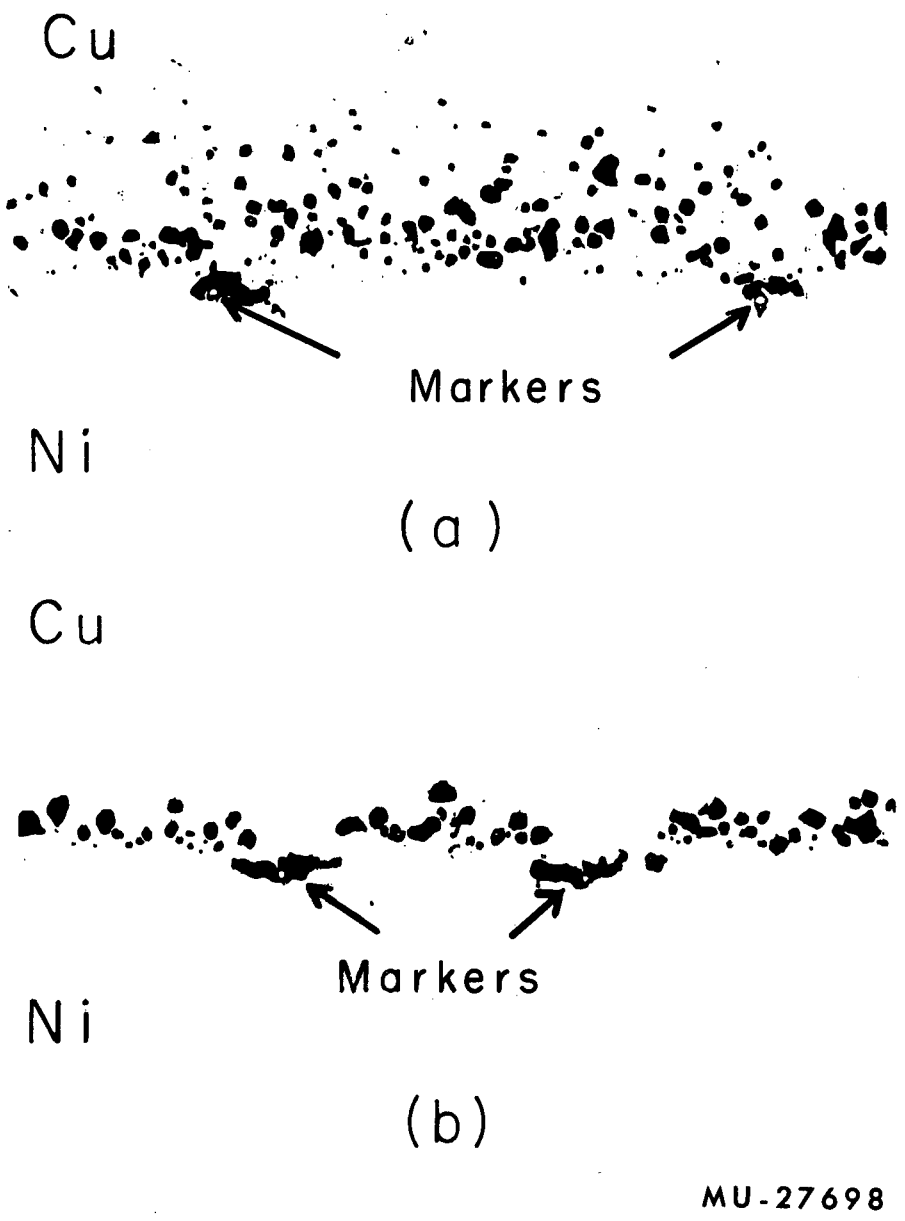

Fig. 4. Effect of interface markers on the distribution of porosity in copper/nickel couples diffused for 720 h at 900°C. Unetched; 70X. (a) OFHC copper/nickel, (b) Spec copper/nickel.

Photomicrographs of electrolytically etched sections showing the distribution of porosity relative to grain boundaries are presented in Fig. 5 and 6. It is evident (Fig. 5) that the location of the porous zone and distribution of pores within this zone is not dependent upon the orientation of the grains nor upon the availability of grain boundaries. This also appeared to be true even at an earlier stage in the formation of porosity, namely after 240 h. Figure 6 shows, at higher magnification, regions in OFHC Cu and Spec Cu in which an unusually high concentration of pores was observed at grain boundaries. A more typical distribution, however, is shown in Fig. 7 which represents a section parallel to the original weld interface near the position of the markers in an OFHC Cu/Ni couple.* Pores are observed both at grain boundaries and within the grains themselves, and the scale on which the porosity is distributed is obviously much finer than the average grain size. Thus, while there may be some slight tendency for pores to form preferentially at grain boundaries, this preference is not very pronounced.

Pores are also found occasionally at twin boundaries, as illustrated in Fig. 8. The crystallographic nature of some of these pores is particularly evident in this figure.

By areal analysis, it was found that after 720 h of diffusion the pores accounted for a total of 16% of the volume of the porous zone in OFHC Cu and 23% in Spec Cu. Considering the width of the porous zone, (See Table IV) these values correspond to a total pore volume of 5.8×10^{-3} cm^3 per cm^2 and 3.0×10^{-3} cm^3 per cm^2 for OFHC Cu and Spec Cu, respectively.

---

*This couple fell apart during machining after having been diffused for 296 h at 900°C.

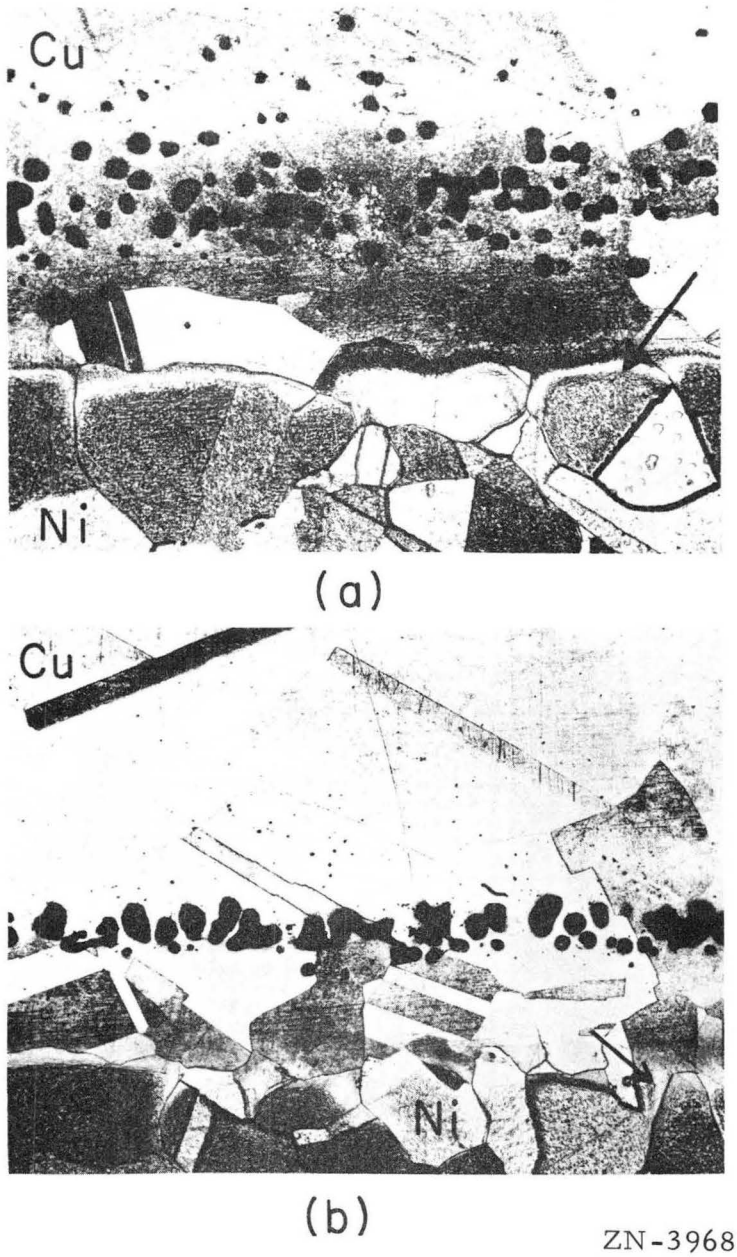

Fig. 5. Electrolytically etched cross sections of copper/nickel couples showing the distribution of porosity relative to the grain boundaries. Arrow indicates position of etch limit. Note evidence for preferential penetration of copper along grain boundaries on the nickel side. Couples diffused for 720 h at 900°C. 100X. (a) OFHC copper/nickel, (b) Spec copper/nickel.

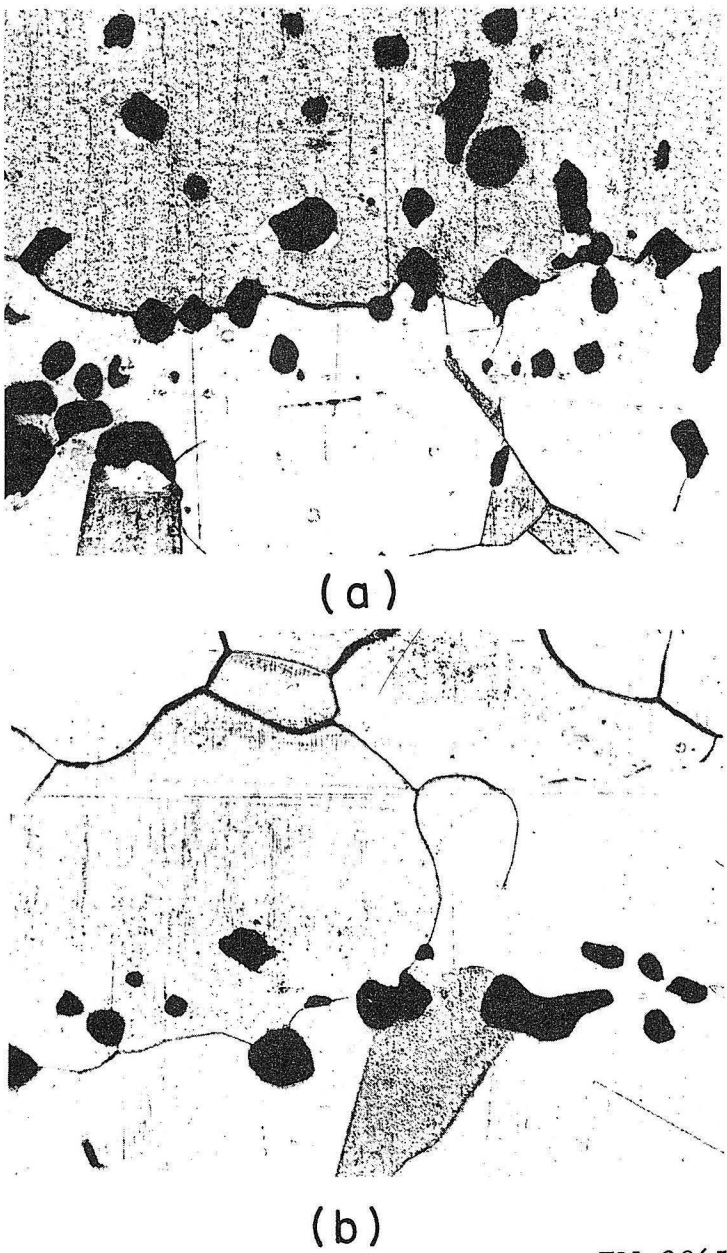

Fig. 6. Photomicrographs illustrating the presence of cavities at grain boundaries as well as within the grains. Couples diffused 720 h at 900°C. Electrolytically etched; 215X. (a) OFHC copper/nickel, (b) Spec copper/nickel.

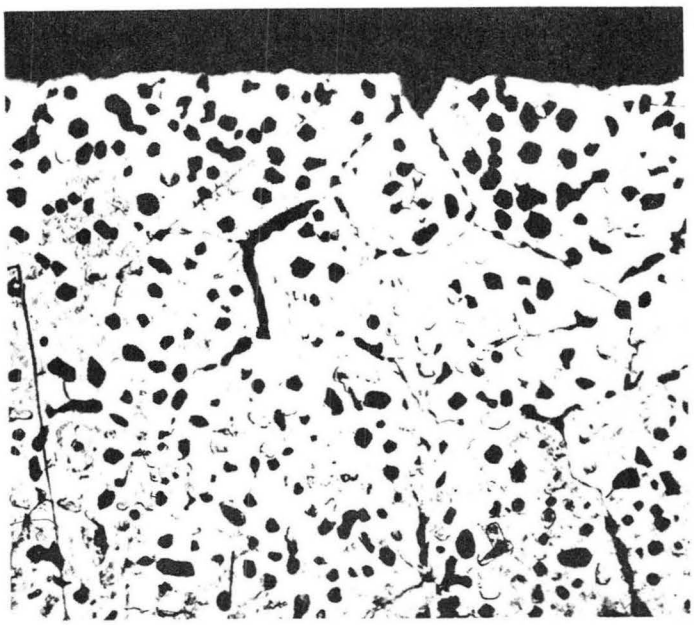

ZN-3210

Fig. 7. Distribution of porosity in a plane parallel to the weld interface near the position of the markers in an OFHC copper/nickel couple diffused for 296 h at 900°C. Unetched; 165X.

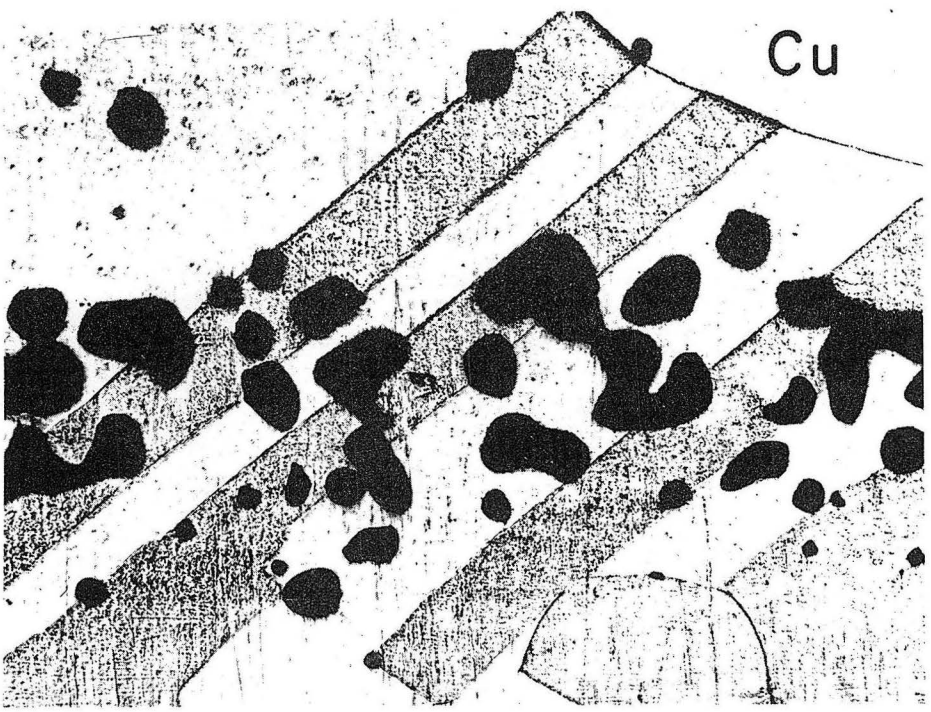

ZN-3967

Fig. 8. Porosity observed within a heavily twinned region in an OFHC copper/nickel couple after diffusion for 720 h at 900°C. Electrolytically etched; 275X.

2. Ag-Au System

The general appearance of the porosity formed in Ag (99.999%)/Au couples is shown in Fig. 9. The nature of porosity in this system appears to be somewhat different from that found in Cu/Ni couples. Instead of being roughly spherical in shape, the voids appear to be elongated and interconnected by "channels". As in the Cu-Ni system, the amount of porosity and the width of the porous zone increased progressively with time. In general, the observations were entirely consistent with those made by previous investigators.[7,9,12,16,18,19,22] However, the porosity seen in couples prepared from the internally oxidized silver alloy presented a distinctly different appearance from that observed in pure silver. A spongy layer in which the porosity was distributed on a scale almost too fine to be resolved in the microscope was found near, but still displaced from, the marker interface. Even after the most careful polishing, it was difficult to obtain a true indication of the structure of this spongy layer. It did appear to be quite brittle, however, and the spongy material was easily broken away during polishing.

Isolated pores of macroscopic size were found beyond this spongy region, i.e., at distances further removed from the interface. These pores were quite crystallographic in nature as distinct from the more rounded and elongated voids found in relatively pure silver. The crystallographic nature of the porosity in this case may be related to the fact that the silver matrix was saturated with oxygen. It is known, for example, that silver evaporates more readily in an oxygen containing atmosphere than in an inert atmosphere;[41] it is also possible that the presence of oxygen might accentuate the anisotropy in surface energies.[42]

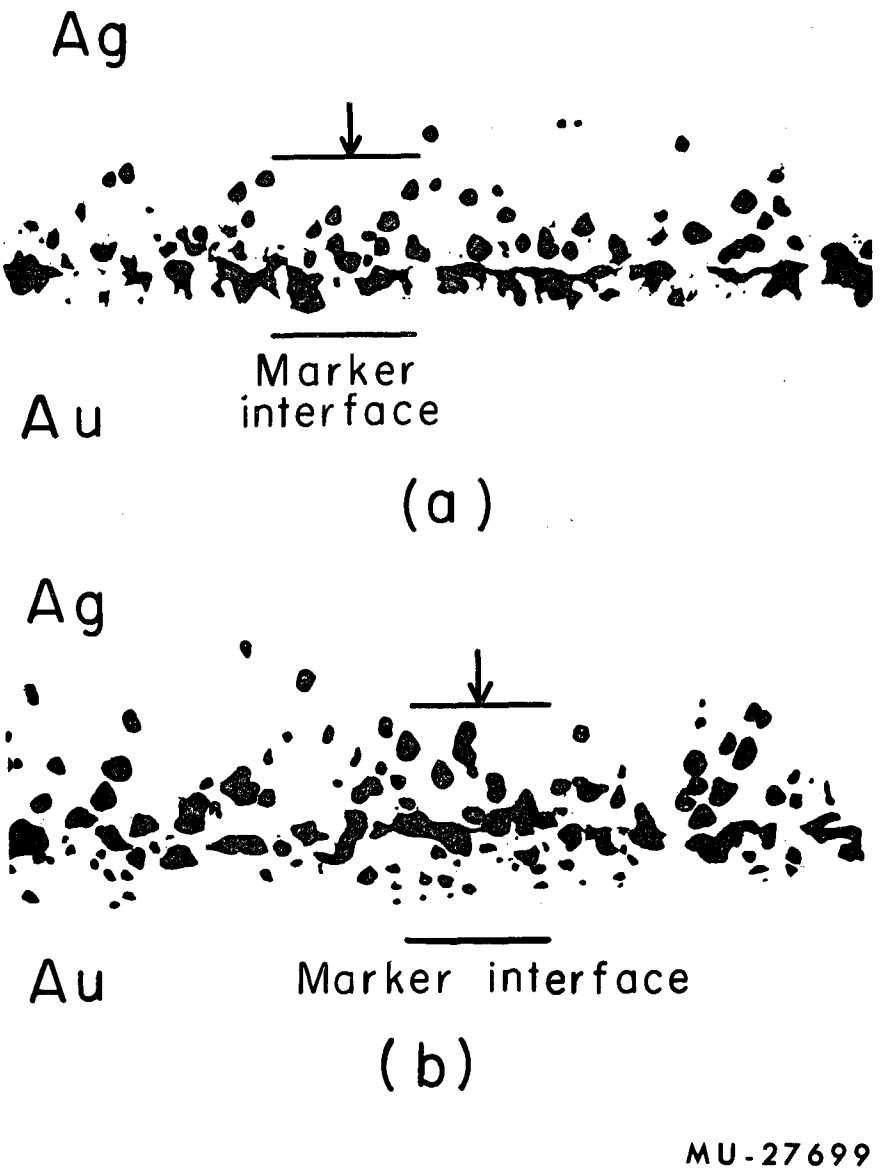

Fig. 9. Distribution of porosity in a silver (99.999%)/gold couple diffused at 875°C. Arrow indicates limit of porous region. Unetched; 120X. (a) 25 h, (b) 50 h.

B. Surface Topography of Diffusion Couples

The structure which developed on surfaces perpendicular to the weld interface in copper/nickel couples after heating in argon for 240 h at 900°C (total diffusion time = 720 h) is shown in Fig. 10. The following features are evident:

(1) Pores which were originally present on the polished surface or which may have broken through the surface during the diffusion anneal.

(2) Plastic deformation within the diffusion zone, as evidenced particularly by recrystallization and by the surface rippling which appears on both the nickel-rich and copper-rich sides of the interface.

Barnes[17] has made a detailed study of surface rippling in the Cu-Ni system and found that the direction of the ripples in each grain corresponds with the intersection of a {110} plane with the surface. He concluded that the surface rippling is a direct result of volume diffusion and he associated the rippling with the climb of dislocations.

More recently, a study of such surface effects was made on single crystals by Ruth.[59,60] Gold-silver alloy couples (i.e., 68 wt % Au - 32 wt % Ag vs. 18 wt % Au - 82 wt % Ag) were employed. In agreement with the work of Barnes,[17] the ripples on the gold-rich side were found to correspond with the intersection of a {110} plane with the surface, but rippling was only observed in those regions where a <112> direction intercepts the surface and passes through the specimen axis. It was concluded that, on the gold-rich side, excess atoms are accommodated either at jogs on edge dislocations, thus resulting in dislocation climb in the {110} plane, or at the crystal surface as a result of rapid diffusion along the so-called "dislocation pipes". The

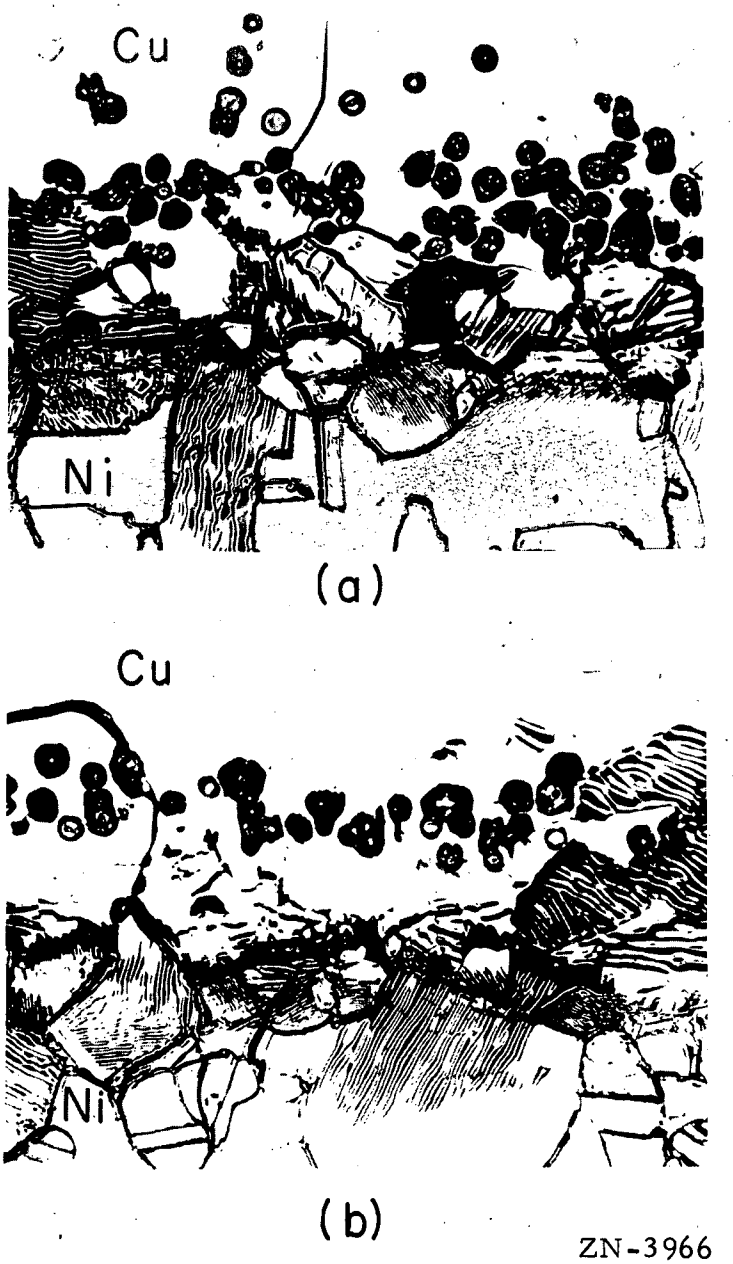

Fig. 10. Structure developed on the surface of copper/nickel couples after heating in argon for 240 h at 900°C (total diffusion time 720 h). 100X. (a) OFHC copper/nickel, (b) Spec copper/nickel.

combined effects of dislocation climb and pipe diffusion would produce surface protusions. Subsequent sintering could then cause these protrusions to take the form of ripples with the observed orientation. Recrystallization in the diffusion zone on the silver-rich side made it impossible to carry out a similar analysis. Nevertheless, it was felt that the same mechanism, except opposite in sense, could account for the rippling observed on this side of the diffusion couple.

The surface topography of the gold-silver couples has also been examined and the structual features which have been observed are vitually identical to those described by Ruth.[22,60] It is believed, therefore, that a substantial amount of diffusion occurred even in those couples that ultimately fell apart. In our case, however, it is likely that a significant part of this diffusion took place by transport through the vapor phase across the incompletely welded silver-gold interface.

C. Dimensional Changes and Motion of Porous Zones

1. Cu-Ni System

The normal Kirkendall shifts for Spec Cu/Ni and OFHC Cu/Ni are plotted as a function of the square root of the diffusion time in Fig. 11. Each point represents the average of 15 individual measurements, the spread in these values being indicated by the vertical bar through each point. The straight lines shown have been calculated by the method of least squares. In both systems the interface marker movement appears to be adequately described by a parabolic time law of the form

$$\Delta = a\sqrt{t} + b,$$

where

a = the slope of the line

b = the intercept along the "displacement" axis.

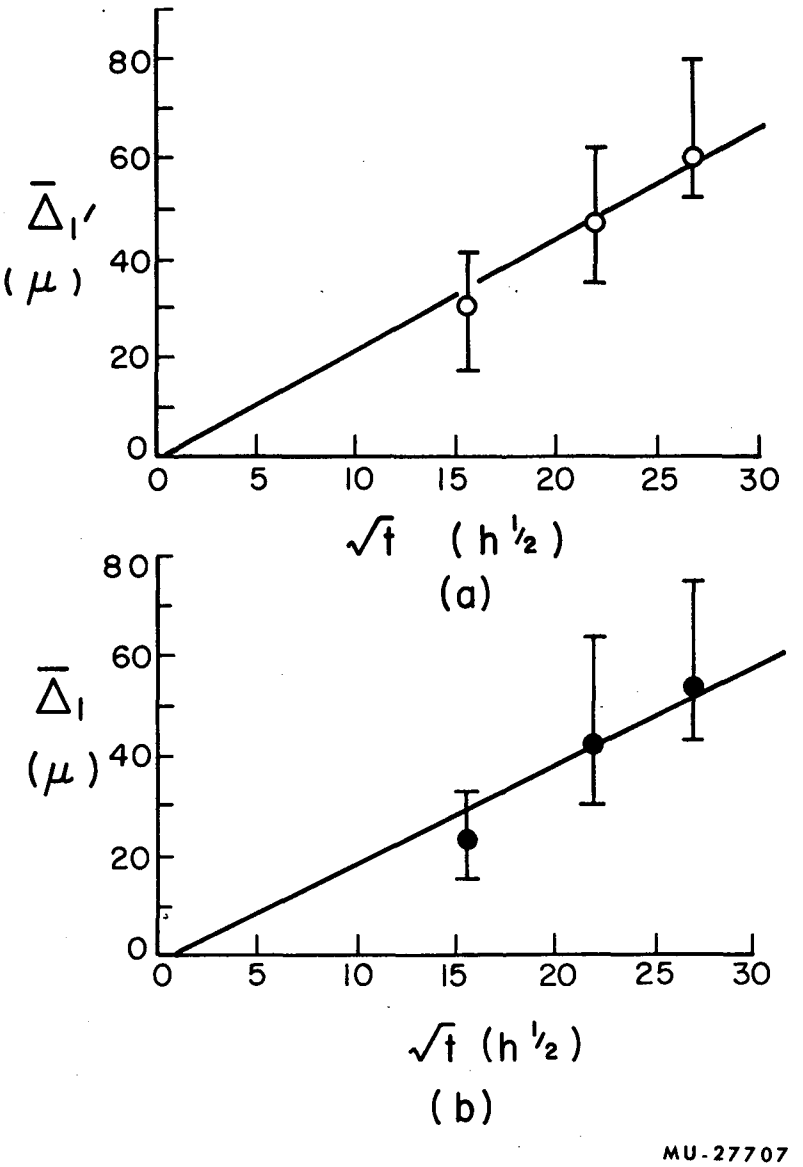

Fig. 11. The normal Kirkendall shift as a function of the square root of the diffusion time at 900°C. Each point represents the average of 15 measurements. (a) OFHC copper/nickel, (b) Spec copper/nickel.

The values of the slope derived from the least square lines are 2.2 μ-hr$^{-1/2}$ for OFHC Cu/Ni; 2.0 μ-hr$^{-1/2}$ for Spec Cu/Ni. The fact that the lines do not pass through the origin may simply indicate that a finite time is required before the steady-state concentration at the marker interface is established.

The observed dimensional changes in the direction of diffusion are summarized in Table III. For a given time of diffusion, the overall expansion is considerably smaller in Spec Cu than in OFHC Cu. The ratio of the average overall expansion to the average Kirkendall shift, $\bar{\Delta}_2/\bar{\Delta}_1$, is also shown in Table III. It is evident that in both cases the overall expansion represents a significant fraction of the normal Kirkendall shift, $\bar{\Delta}_2/\bar{\Delta}_1$ being approximately twice as large in OFHC Cu than in Spec Cu. After 720 h of diffusion, for example, this ratio is 0.87 for OFHC Cu and 0.45 for Spec Cu. $\bar{\Delta}_2/\bar{\Delta}_1$ appeared to be constant with time in Spec Cu but decreased from 1.2 after 240 h to 0.87 after 720 h in OFHC Cu.

The measured expansions after 720 h:

$$\bar{\Delta}_2 = 2.4 \times 10^{-3} \text{ cm}$$

$$\bar{\Delta}_{2'} = 5.2 \times 10^{-3} \text{ cm}$$

are in good agreement with the expansion calculated from the total pore volume, i.e., 3.0 x 10^{-3} cm^3 per cm^2 and 5.8 x 10^{-3} cm^3 per cm^2 for Spec Cu/Ni, and OFHC Cu/Ni, respectively, on the assumption that the dimensional changes resulting from the formation of porosity are entirely confined to the direction of diffusion. This assumption appears to be justified experimentally. Measurements have been made of the lateral dimensional changes, i.e., the distance between adjacent markers at a given interface, and these have been found to be negligible within the uncertainty of the measurements ($\pm$ 2μ). Other investigators[4,12,16] have also reported that in massive diffusion couples the dimensional changes transverse to the

TABLE III Dimensional Changes in OFHC Cu/Ni and Spec Cu/Ni Couples Diffused at 900°C

Diffusion Time Hours	Components	Kirkendall shift Δ_1, μ			Overall expansion Δ_2, μ			Contraction on the Cu Side Δ_3, μ			$\bar{\Delta}_2/\bar{\Delta}_1$
		min	max	ave	min	max	ave	min	max	ave	
240	OFHC Cu/Ni	+17	+39	+30	+27	+42	+35	+16	- 6	+ 5	1.20
	Spec Cu/Ni	+16	+33	+23	+ 6	+19	+10	- 2	-29	-13	0.43
480	OFHC Cu/Ni	+26	+58	+47	+25	+56	+44	+ 8	-25	- 3	0.94
	Spec Cu/Ni	+26	+64	+42	+ 9	+27	+18	- 7	-48	-24	0.43
720	OFHC Cu/Ni	+44	+81	+60	+41	+64	+52	+ 8	-23	- 8	0.87
	Spec Cu/Ni	+44	+68	+53	+12	+41	+24	-10	-50	-29	0.45

TABLE IV Motion of the Zone of Porosity
(Values represent average of 15 measurements)

Time (h)	Measured Quantity	OFHC Cu/Ni, μ	Spec Cu/Ni, μ
480	Displacement of boundary I	83	72
	Displacement of boundary II	360	175
	Width of porous zone	286	103
	Distance between interface marker and boundary I	36	30
720	Displacement of boundary I	108	93
	Displacement of boundary II	465	222
	Width of porous zone	357	129
	Distance between interface marker and boundary I	48	40

diffusion direction are extremely small -- of the order of 0.2 - 0.7%.

In Fig. 12, the average overall expansion and the average contraction on the copper side are shown as a function of the square root of the diffusion time. Like the normal Kirkendall shift, $\bar{\Delta}_2$ and $\bar{\Delta}_3$ exhibit a $t^{1/2}$ time dependence for both OFHC and Spec copper. However, the least square lines through the data for $\bar{\Delta}_2$ and $\bar{\Delta}_3$, if extrapolated to zero time would not coincide with the extrapolation for $\bar{\Delta}_1$. The reason for this discrepancy is not known, nor can any explanation be given at present for the fact that the overall expansion in OFHC Cu/Ni after 240 h is greater than the expansion on the nickel side.

It will be noted from Table III, in which the minimum and maximum shifts are also listed, that the scatter in the measured marker displacements is quite large - significantly larger, in fact, than the uncertainty in any individual measurement. Wide variations of this sort have commonly been observed in the past.[4,19] It appears from the data that the behavior of individual markers is qualitatively similar to the average, in that the displacement of any individual marker increases parabolically with time. No correlation was found between the marker environment (i.e., the size of the void surrounding the marker, the distribution of porosity in the vicinity of the marker or the proximity of the marker to grain boundaries) and the actual extent of the marker shift. As will be shown, however, there did appear to be consistent differences in the amount of diffusion which occurred locally near the markers exhibiting the minimum and maximum shifts.

The position of the porous zone with respect to the Cu-Ni interface and the average width of this zone was determined after 480 and 720 h in OFHC Cu/Ni and Spec Cu/Ni. The results of these measurements are listed in Table IV. The average displacements of the boundaries of the porous

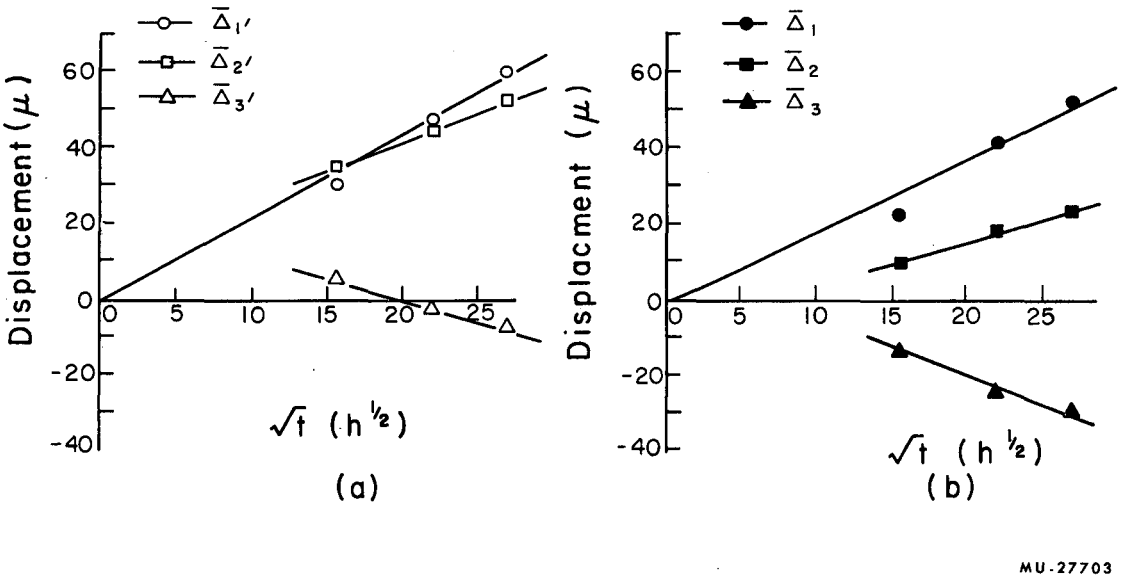

Fig. 12. Average dimensional changes in the diffusion direction. The normal Kirkendall expansion ($\bar{\Delta}_1$), the over-all expansion of the couple ($\bar{\Delta}_2$), and the contraction on the copper side ($\bar{\Delta}_3$) are shown as a function of the square root of the diffusion time at 900°C. (a) OFHC copper/nickel, (b) Spec copper/nickel.

zone are plotted as a function of the square root of the diffusion time in Fig. 13. In Spec Cu, as well as OFHC Cu, both boundaries of the porous zone migrate parabolically with time in a direction away from the original marker interface. The average width of the porous region also appears to increase approximately as $t^{1/2}$ in both cases. The porous zone in OFHC Cu is about three times as wide in Spec Cu and this ratio, $W_{\text{OFHC Cu}}/W_{\text{Spec Cu}}$, remains approximately constant with time.

The nickel-rich boundary (I) of the porous zone has actually moved away from the Kirkendall interface in both OFHC Cu and Spec Cu. This behavior had not previously been observed in the Cu-Ni system, although it had been found in the Ag-Au system; the motion of the porous zone away from the interface has been attributed to elimination of the finely distributed porosity formed early in the diffusion process by a sintering mechanism.[9,12]

It should be noted that the porosity does not always end at a sharply defined plane, especially in OFHC Cu/Ni, but instead a few widely separated pores appear considerably beyond the zone of maximum porosity. In this case, the position at which the majority of the pores ceased to form was taken as the outermost limit of the porous zone.

2. Ag-Au System

Silver-gold couples which showed all of the surface characteristics that are believed to be associated directly or indirectly with volume diffusion,[22] and which subsequently fell apart in the later stages of the diffusion cycle, also exhibited marker motion that obeyed a parabolic time law. The dimensional changes observed in Ag (99.999%)/Au couples were similar in nature to those found in Spec Cu/Ni, namely, $\bar{\Delta}_1 > \bar{\Delta}_2$ and $\bar{\Delta}_2/\bar{\Delta}_1 \cong 0.3 - 0.6$. The magnitude of the observed Kirkendall shift ($a \cong 5\mu - hr^{-1/2}$) is in reasonable agreement with the values reported by

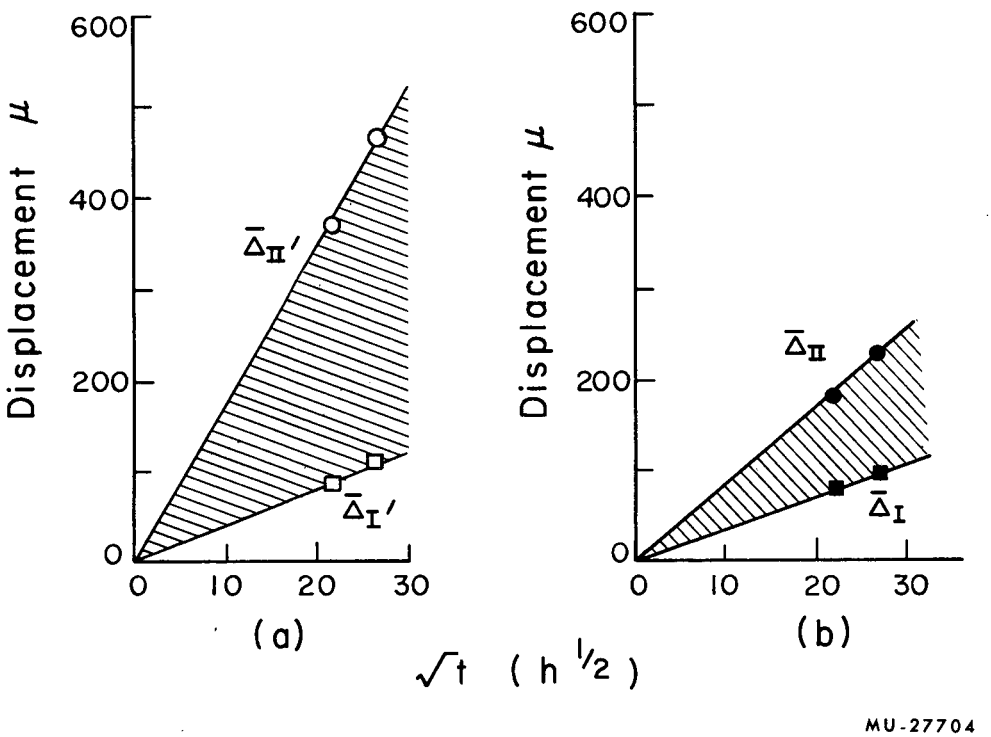

Fig. 13. The average displacement of the zone of porosity as a function of the square root of the diffusion time at 900°C. The crosshatched area represents the average width of the porous zone. (a) OFHC copper/nickel, (b) Spec copper/nickel.

Seith and Kottmann,[10] and Heumann and Walther[19] when appropriate account is taken of the different diffusion temperatures employed by these investigators.

On the other hand, in internally oxidized silver-gold couples, $\tilde{D}_2' > \tilde{D}_1'$ and $\tilde{D}_2'/\tilde{D}_1' \sim 1.0 - 1.3$. In addition, the normal Kirkendall shift ($a \cong 25\ \mu - h^{-1/2}$) was much greater than that in Ag (99.999%)/Au. Whether or not the observed differences between couples prepared from the internally oxidized silver alloy and 5-9's silver are real is difficult to say in view of the fact that many of these couples were not completely welded.

On polished sections of the Ag-Al-O/Au couples there was evidence that grain boundary cracking had occurred on the silver side.* To determine if this had influenced the dimensional changes, three identical pieces of the oxidized alloy were welded together with tungsten wire markers at the respective interfaces and the relative displacements of the markers were measured after diffusion at 875°C. The observed marker movements were far too small to account for the dimensional changes in the Ag-Al-O/Au couples.

D. Concentration-Penetration Curves

The data obtained from the microprobe step-scan analysis (see Appendix) were plotted on probability paper. This permits the tails of the c-x curves to be defined with much greater confidence than would be possible by plotting the concentration profiles directly. The "smooth" probability curve was then transformed to regular rectangular coordinates and plotted in the usual manner as in Fig. 14. The experimental points are represented in Fig. 14 by circles.

From the concentration-penetration curves, it is possible to determine the mass flux of both constituents across the original weld interface.

---

* This may possibly have been accentuated by polishing.

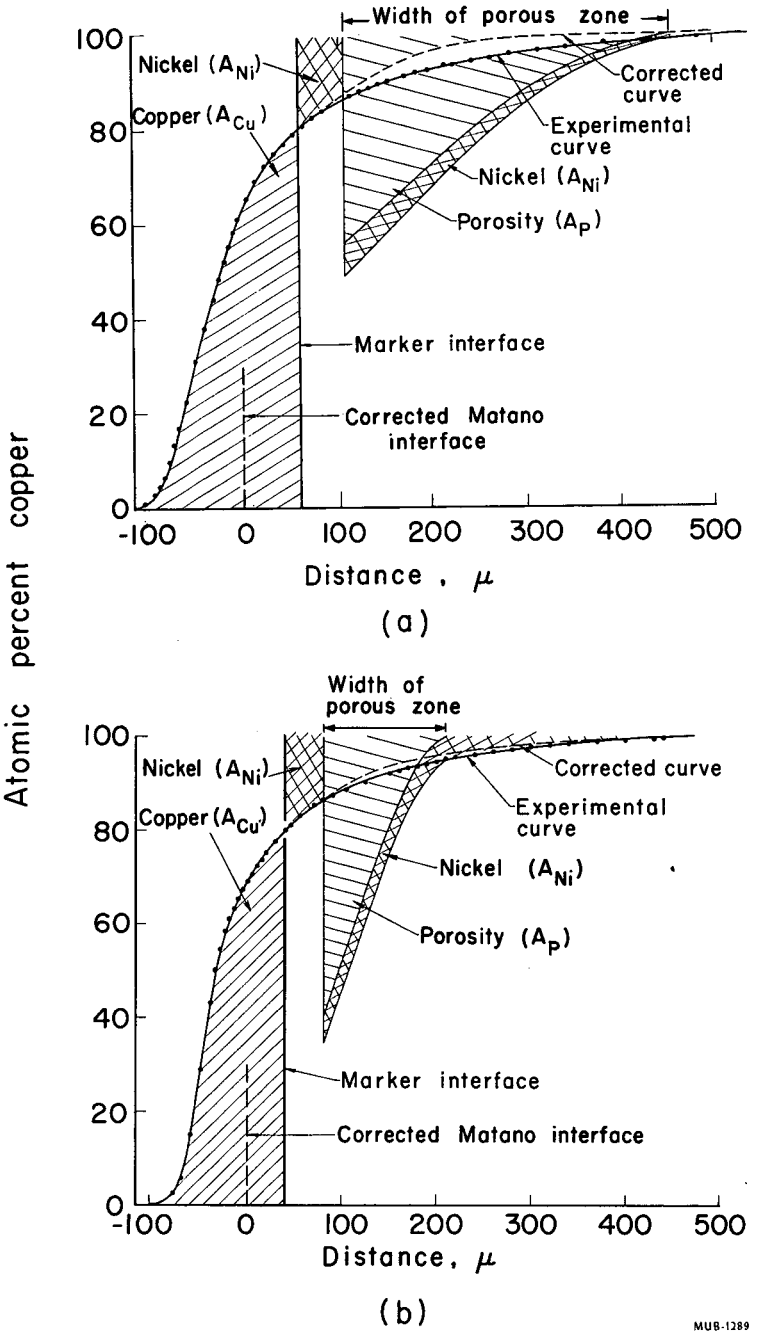

Fig. 14. Concentration-penetration curves derived from microprobe analysis; corrections to the C-X curves due to the presence of porosity are indicated. The amount of porosity on the copper-rich side, and the amount of nickel diffused into the copper side and the amount of copper diffused into the nickel side across the original interface are represented by the crosshatched areas. (a) OFHC copper/nickel (b) Spec copper/nickel.

Before this can be done, however, the c-x curves must first be corrected for the presence of porosity. This correction is also required in the calculation of D_{chem} as a function of composition since changes in density invalidate the usual solutions to the diffusion equation.[43] The porosity correction has been made in accordance with the method outlined by Balluffi.[44] For this purpose the distribution of porosity as a function of distance from the Kirkendall interface was determined by lineal analysis from photographs.* The corrected c-x curves are shown in Fig. 14. The amount of porosity formed on the copper side and the amount of nickel whichdiffused across the marker interface are represented by the hatched areas.

The area A_{Cu} under the c-x curve lying to the left of the marker (i.e., Kirkendall) interface is proportional to the number of copper atoms which have diffused across the interface into the nickel side. Similarly, the area A_{Ni} lying above the corrected c-x curve to the right of the marker interface is proportional to the atom flux of nickel. The difference between these two quantities should therefore represent the net flux of vacancies into the copper side. These quantities are given in Table V, the values listed being based on unit area of interface. In Table V, A_p corresponds to the amount of porosity obtained from linear analysis. Thus, the ration, $A_p/A_{Cu}-A_{Ni}$, should be a measure of the fraction of the net number of vacancies which end their lives at pores.

Values of the chemical diffusivity at selected compositions were then calculated from the corrected c-x curves by applying the Boltzmann-Matano[45] analysis. D_{chem} is plotted as a function of composition in Fig. 15. The errors in calculating the chemical diffusion coefficient are greatest at the extremes of the composition range where there is the largest uncertainty in

* The total pore volume derived from linear analysis agreed very closely with that obtained previously by areal analysis.

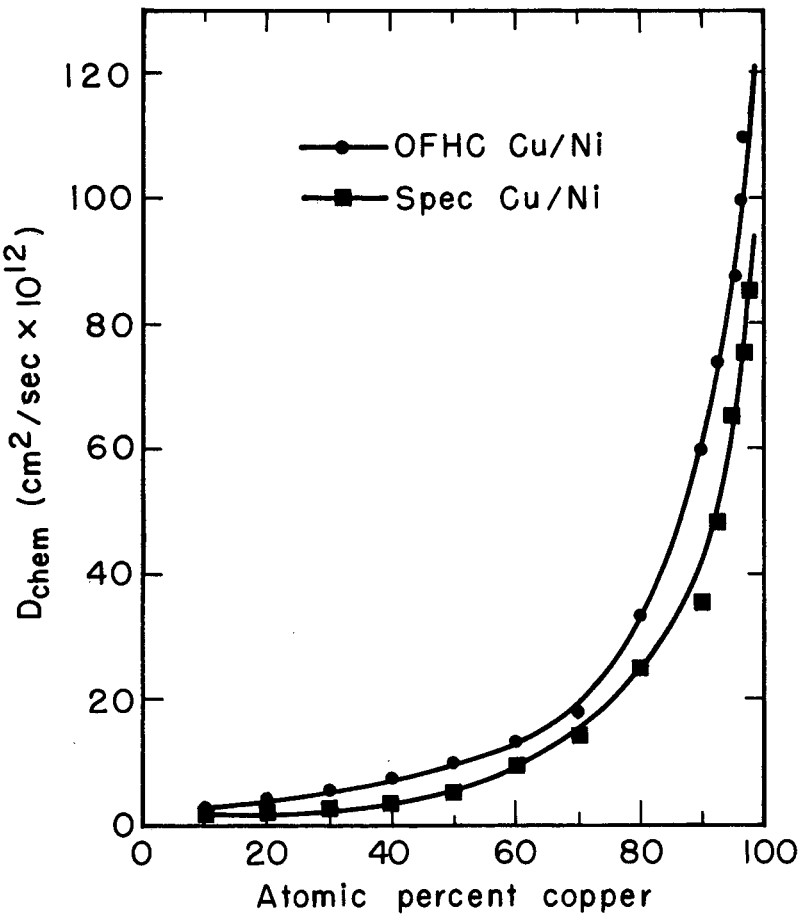

Fig. 15. Chemical diffusion coefficient as a function of concentration for OFHC copper/nickel and Spec copper/nickel at 900°C.

TABLE V Relative Amounts ($cm^3/cm^2 \times 10^3$) of Copper and Nickel Diffused Across the Marker Interface

Components	A_{Cu}	A_{Ni}	$A_{Cu}-A_{Ni}$	A_P	$A_P/A_{Cu}-A_{Ni}$
OFHC Cu/Ni	7.6	1.3	6.3	6.0	0.95
Spec Cu/Ni	6.2	2.0	4.2	3.0	0.71

determining the exact slope of the c-x curve. Consequently, near the copper-rich end, D_{chem} was calculated at a number of closely spaced intervals, and the best smooth curve was drawn through the resulting points. Differences in the molar volumes of the diffusing components and variations of these molar volumes with composition have been neglected. No appreciable change in the overall volume of the couple would be expected in the Cu-Ni system since the molar volume is virtually a linear function of the atomic fraction.[46] If the volume of nickel, 3.3×10^{-3} cm^3 per cm^2, represented by the Matano area in the case of OFHC Cu/Ni (see Fig. 14a) is replaced by an equal number of copper atoms, the volume increases to 3.6×10^{-3} cm^3 per cm^2. The difference, 3.0×10^{-4} cm^3 per cm^2, corresponds to a displacement of the Matano interface of 3 μ. This shift can be neglected compared to the accuracy of the penetration measurements (~ ± 2 μ) and the approximate nature of the correction made for the expansion of the couple resulting from the formation of porosity.

The intrinsic diffusion coefficients D_{Cu} and D_{Ni}, corresponding to the concentration at the marker interface (1 and 1') were then calculated from the Darken equations:

$$v = (D_{Cu} - D_{Ni}) \frac{dN_{Cu}}{dx} \qquad (9)$$

and $$D = N_{Ni} D_{Cu} + N_{Cu} D_{Ni}, \qquad (10)$$

where

v = average marker velocity

N_{Cu} = atomic fraction of copper

N_{Ni} = atomic fraction of nickel

$\frac{dN_{Cu}}{dX}$ = concentration gradient

D = chemical diffusion coefficient corresponding to the composition at the markers.

The average marker velocity was calculated from the marker displacements $\bar{\Delta}_1$ and $\bar{\Delta}_1$, according to the relation:[48]

$$v = \frac{\bar{\Delta}_1}{2t} \qquad (11)$$

The derived values of D_{Cu} and D_{Ni} and the ratio D_{Cu}/D_{Ni} are listed in Table VI together with the concentration at the average marker interface (1 and 1').

TABLE VI Intrinsic Diffusivities in the Cu-Ni System at 900°C

Components	Composition at markers, N_{Cu}	Chemical diffusivity, D_{chem} (cm^2/sec)	Intrinsic diffusivities (cm^2/sec)		$K = \frac{D_{Cu}}{D_{Ni}}$
			D_{Cu}	D_{Ni}	
OFHC Cu/Ni	0.800	3.3×10^{-11}	9.0×10^{-11}	1.9×10^{-11}	4.7
Spec Cu/Ni	0.793	2.4×10^{-11}	5.8×10^{-11}	1.5×10^{-11}	3.9

The concentration-distance profiles obtained at the position of the interface markers which exhibited the minimum and maximum Kirkendall shifts after 720 h of diffusion at 900°C are given in Figs. 16 and 17. Aside from disturbances in the microprove analysis due to the presence of porosity (Fig. 16) the profiles obtained on the copper-rich side are virtually the same at both

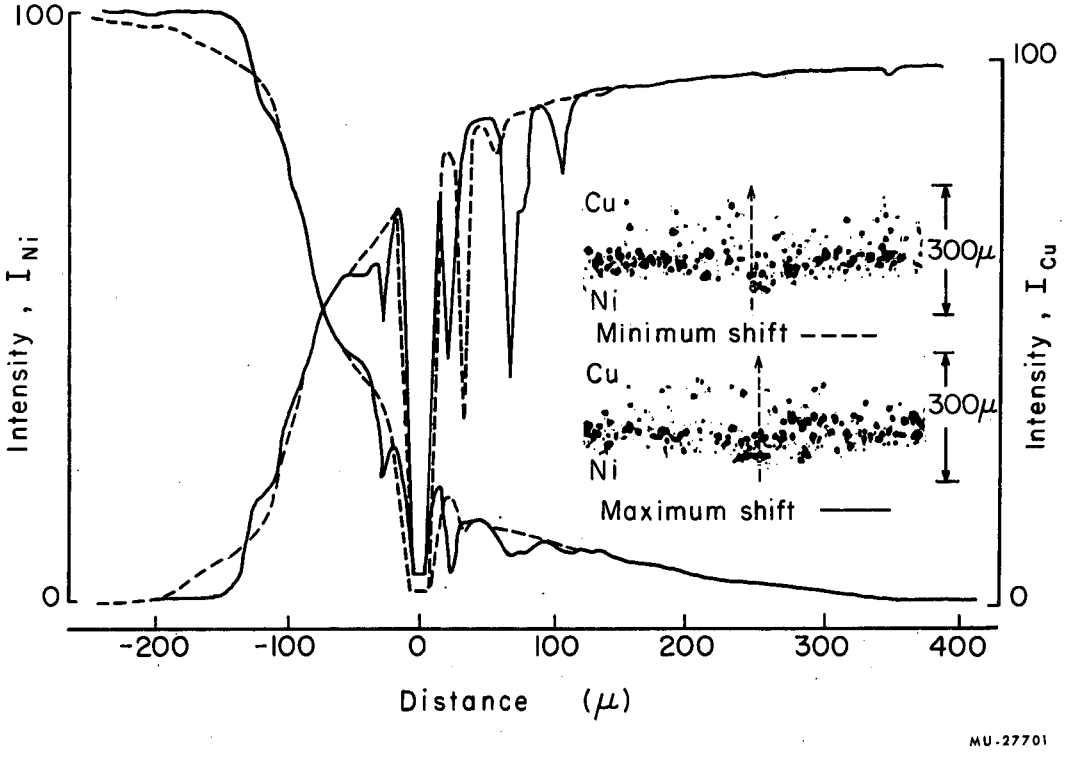

Fig. 16. Concentration-penetration profiles for a OFHC copper/nickel couple diffused 720 h at 900°C. Uncorrected x-ray intensities (normalized) are plotted as a function of distance from those interface markers that exhibit the maximum and minimum displacements. The photomicrographs (inset) show the distribution of porosity at these two positions. The intensities were scanned in the directions indicated by the dashed lines on the photographs.

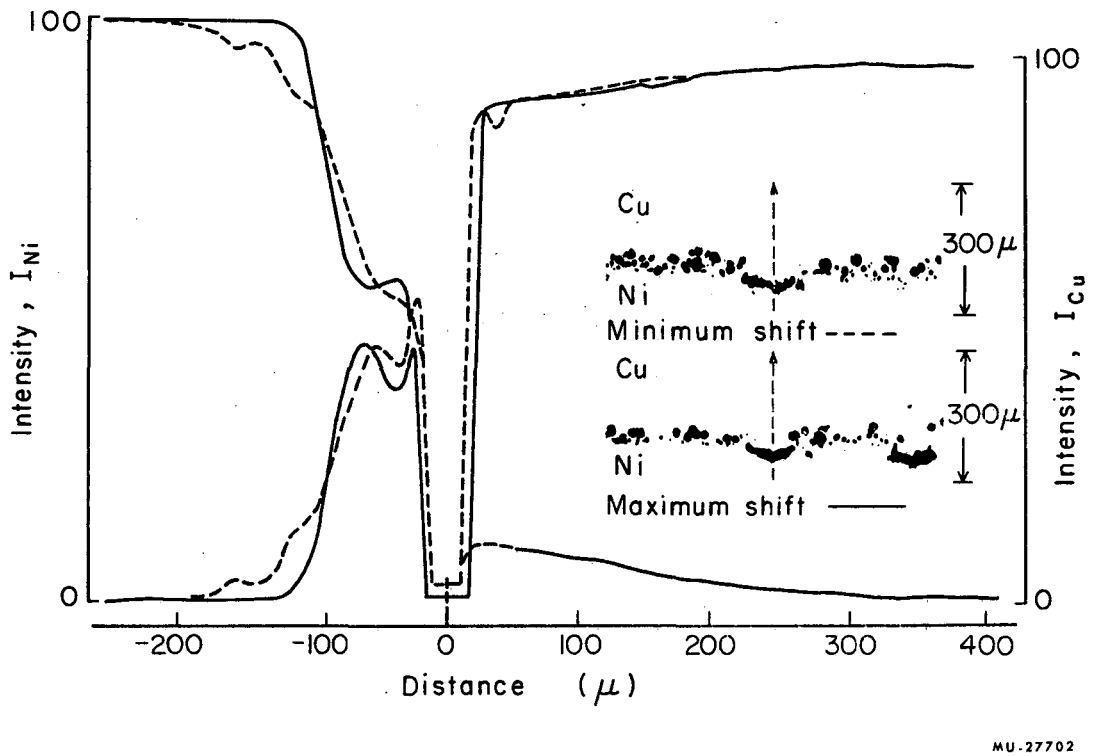

Fig. 17. Same as Fig. 16 except for a Spec copper/nickel couple diffused 720 h at 900°C.

these marker positions in OFHC Cu as well as Spec Cu. On the nickel-rich side, however, it appears as though a greater amount of diffusion has taken place in the vicinity of the marker which shows the minimum displacement. This same behavior is seen in both OFHC and Spec copper. A measurement of the position of the etch limit (see Fig. 5) relative to these same markers verified that this effect was, in fact, real.*

Concentration profiles obtained on the copper side parallel to the Cu-Ni interface indicated that, at distances of 100 and 200 μ from the marker interface, the composition was essentially constant in both Spec Cu and OFHC Cu.

---

* The position of the etch limit, when related to the corresponding c-x curve, was found to agree with the point of maximum penetration of copper into nickel to within ±2 at %.

IV. DISCUSSION

In the analysis of the data it will be assumed that diffusion takes place by a vacancy mechanism in the two systems investigated, and that the formation of porosity is indeed the result of the condensation of vacancies. Both the dimensional changes and the amount of porosity formed in the diffusion zone will thus be determined by the relative fraction of vacancies that end their lives at pores and at dislocations or other sinks. If all of the excess vacancies created on the copper side of the original interface are annihilated at dislocations, it would be expected that the contraction on the copper side would be approximately equal to the expansion on the nickel side and therefore that the overall expansion would be essentially zero. On the other hand, if the excess vacancies are entirely absorbed at pores, then virtually no contraction would occur on the copper side and the overall expansion of the couple would, to a first approximation, be equal to the normal Kirkendall shift. The experimental observations indicate that the actual behavior lies somewhere between these two extremes and that in OFHC Cu a greater fraction of the vacancies condense to form pores than in Spec Cu.

Estimates of the relative fractions of vacancies which go to pores and to dislocations have been obtained in two ways: (1) from the ratio of the overall expansion to the normal Kirkendall shift (see Table III); and (2) from the ratio of the measured pore volume to that calculated from the net vacancy flux (see Table V). Both estimates are in reasonable agreement and indicate that upwards of fifty percent of the vacancies go to form pores in Spec Cu, whereas perhaps as much as 80 to 90% agglomerate as pores in OFHC Cu. These estimates are based on the assumptions that the atomic volume of a vacancy is equal to the atomic volume of a copper atom and that the

volume occupied by a cluster of n vacancies in a pore is the sum of the volumes of n isolated vacancies (or copper atoms). Recent theoretical and experimental work indicates, however, that the volume occupied by a vacancy in copper may be significantly less than one atomic volume, perhaps as low as 0.5 atomic volumes.[61,62] It would also be expected that the relaxation around a cluster of vacancies might be even greater than that around an isolated vacancy. As a consequence, the fractions of vacancies which end their lives at pores may be actually greater than the estimates obtained from the present measurements.

Barnes[6] estimated, on the basis of the relative expansion and contraction on the two sides of a Cu/Ni diffusion couple, that roughly half of the vacancies condensed into pores, the other half presumably disappearing at dislocations. The copper used by Barnes, although admittedly from another source, was stated to be spectoscopically pure, and might correspond to the spectrographically pure copper used in this investigation. In the same study, Barnes[6] measured the overall expansion as well as the density changes which occurred in multi-layer diffusion couples prepared from both "commercially" pure and spectrographically pure copper sheet. The magnitude of the expansion was significantly greater with commercially pure copper although this was not pointed out by the author. The present observations therefore seem entirely consistent with those of Barnes and suggest that more potent nuclei for vacancy condensation may exist in OFHC Cu than in Spec Cu.

The chemical analyses of the two grades of copper used in this study do not, however, furnish any positive clues concerning the nature of these nuclei. It is seen from the analyses given in Table II that the iron and sulfur concentrations are somewhat higher in OFHC Cu, and it is suspected

that the phosphorus, selenium or tellurium contents may also be higher, since these elements are frequently added to OFHC Cu in order to improve machinability.[50] Hence, some second phase constituent, perhaps a sulfide, selenide, or telluride of a trace impurity such as iron, might possible be present. Such compounds might have the requisite thermodynamic stability at the diffusion temperatures to serve as "effective" nuclei. It is also possible that an oxide may be involved and that the differences in the oxygen concentrations between OFHC and Spec Cu might be sufficient to account for the observed behavior.

Some indication that oxide particles or clusters may act as favorable sites for vacancy condensation is provided by the observations on the nature of the porosity in pure silver and the internally oxidized silver alloys. For example, the very finely distributed porosity seen near the marker interface in the oxidized alloy was absent in pure silver. If the observed dimensional changes in these couples are associated directly with the diffusion process and are not caused by secondary processes, they would also suggest that a greater volume of porosity is formed in Ag-Al-O. Resnick and Seigle[20] reported that in Ag/Au couples prepared from silver having a high concentration of oxygen, the nature of the porosity was altered, presumably by the presence of Ag_2O.

The relative excess concentration of vacancies present in the diffusion zone at the point where pores just cease to form (i.e., boundary II of the zone of porosity) was calculated using an expression derived by Balluffi.[13] The rate at which vacancies accumulate per unit volume within the diffusion zone is given by:[28]

$$\frac{\partial N_v}{\partial t} = - \text{div } I_v - \frac{N_{vo} R}{\tau} , \qquad (12)$$

where N_v is the actual number of vacancies per unit volume, N_{vo} is the equilibrium concentration, $R = (N_v/N_{vo} - 1)$ is the relative excess concentration, I_v is the vacancy current, and τ is vacancy lifetime. By making reasonable approximations, it is possible to obtain an order of magnitude estimate for the ratio R_c/τ corresponding to the conditions under which a stable pore of critical size will be formed. Since the number of vacancies created and annihilated within a unit volume of the diffusion zone will be large compared to the change in the number maintained there, the term $\partial N_v/\partial t$ must be relatively small. In addition, it may be assumed that the motion of the vacancies is largely determined by the pumping action of the chemical activity gradient and not by any vacancy gradients which are established during diffusion. Div I_v may then be approximated by:

$$\frac{\partial}{\partial x} \left[(D_{Cu} - D_{Ni}) \frac{\partial N_{Cu}}{\partial x} \right] , \qquad (13)$$

and assuming that the ratio of intrinsic diffusivities, $K = D_{Cu}/D_{Ni}$, is essentially independent of concentration, Eq. (12) may be rewritten as:

$$\frac{N_{vo}}{N} \frac{R_c}{\tau} \sim \left[\frac{(1 - K)}{N_{Ni} + KN_{Cu}} \right] \left[D \frac{\partial^2 N_{Cu}}{\partial x^2} + \left\{ \frac{\partial D}{\partial N_{Cu}} + D \frac{(1-K)}{N_{Ni} + KN_{Cu}} \right\} \left\{ \frac{\partial N_{Cu}}{\partial x} \right\}^2 \right] \qquad (14)$$

where N is the total number of atoms per unit volume.

The magnitude of the term $(N_{vo}/N)(R_c/\tau)$ in both OFHC Cu and Spec Cu has been calculated from Eq. (14) at the position in the diffusion zone where porosity just ceases to be observed. The right-hand side of the equation has been evaluated from the c-x curves and the corresponding diffusivity data. It should be noted that the application of Eq. (14) assumes that the porous zone is still advancing at the time diffusion is

interrupted; this certainly appears to be the case in the couples studied here. The calculated values for $(N_{vo}/N)(R_c/\tau)$ in Table VII suggest that pores will form when vacancies are pumped into any small region of the diffusion zone at the rate $\left[\text{ div } I_v \sim (-N_{vo}R_c/\tau)\right]$ of about $10^{15}/cm^3/sec$ in OFHC Cu and $10^{17}/cm^3/sec$ in Spec Cu. The higher supersaturations required for the nucleation of pores in Spec Cu than in OFHC Cu are consistent with all of the qualitative observations on the formation of porosity. It is believed that these differences can be explained in terms of the nature and number of effective nuclei that are present in the two grades of copper.

In order to obtain a numerical value for R_c itself, the quantity $\frac{N_{vo}}{N\tau}$ must be approximated. Simmons and Balluffi[61] have determined the equilibrium concentration of vacancies in copper by a technique involving simultaneous measurement of the linear macroscopic expansion, $\Delta L/L$, and the X-ray lattice parameter expansion, $\Delta a/a$, during equilibrium heating. No knowledge of the volume relaxation around the vacancy is required since this relaxation contributes equally to $\Delta L/L$ and $\Delta a/a$. The measurements yield a value of N_{vo}/N of 3×10^{-5} at 900°C.

A reasonable upper limit for the lifetime of a vacancy can be estimated by assuming that at the diffusion temperature only dislocation jogs are effective sinks for vacancies. With a total dislocation density of $10^7/cm^2$ and assuming that one site in every 1000 along a dislocation line is an effective sink, a vacancy would take on the average 10^{11} jumps before being annihilated. The vacancy lifetime under these conditions is at most 1 sec since:[62]

$$\tau = \frac{n_j}{12\,\nu} \cdot \exp\,(-S^m/k) \cdot \exp\,(E^m/kT) \qquad (15)$$

TABLE VII Data for the Determination of the Relative Excess Concentration of Vacancies Necessary for Pore Formation

Components	Composition at boundary II of the porous zone		$\frac{\partial N_{Cu}}{\partial x}$	$\frac{\partial^2 N_{Cu}}{\partial x^2}$	D_{chem}, cm^2/sec	$\frac{\partial D}{\partial N_{Cu}}$	$K = \frac{D_{Cu}}{D_{Ni}}$	$\frac{N_{vo}}{N} \frac{R_c}{\tau}$
	N_{Cu}	N_{Ni}						
OFHC Cu/Ni	0.995	0.005	0.40	- 94	1.3×10^{-10}	1.4×10^{-9}	4.7	9.6×10^{-9}
Spec Cu/Ni	0.95	0.05	3.6	-864	7.0×10^{-11}	6.5×10^{-10}	3.9	4.8×10^{-7}

where n_j is the average number of jumps a vacancy takes in its lifetime, ν is the characteristic atomic frequency (taken to be the Debye frequency), S^m is the vibrational entropy of motion of a single vacancy (assumed to be 2R),[62] E^m is the energy for motion of a single vacancy (~0.88 ev for copper),[61] k is the Boltzmann constant, and T is the temperature. These values for $\frac{N_{vo}}{N}$ and τ lead to critical supersaturations of 0.0003 in OFHC Cu and 0.02 in Spec Cu. Both values are in the range of supersaturations reported previously by Balluffi and others.[13,18,21] It has been shown that vacancy supersaturations of the order of 1% are required for an unextended edge dislocation to act continuously as a sink for vacancies by a climb process.[27,29] Even if such supersaturations existed within the diffusion zone (as appears to be the case in the Spec Cu/Ni couple), climb would be more difficult in copper because the dislocations are, in general, extended. This means that the partials cannot move out of their slip plane without creating a sizeable surface energy misfit. The amount of misfit will depend on the extent to which dislocation jogs are dissociated and therefore upon the stacking fault energy (40 ergs/cm^2 or 70 ergs/cm^2 in copper).[51,52] The exact geometry of jogs associated with extended dislocations is still quite uncertain.[62-67] Nevertheless, a supersaturation in excess of 1% would most probably be required in order for the dislocations in copper to move in a non-conservative fashionand thereby function as effective vacancy sinks.

Other things being equal, the relative fraction of vacancies which end their lives at pores and at dislocations will be determined, at least in part, by the ease with which dislocations climb. Hence, any factor which makes climb more difficult will favor pore formation, assuming that the density of nuclei is not changed. One would therefore expect to find

large amounts of porosity in both Spec Cu and OFHC Cu, which is in agreement with observations. Whether or not the observed differences in porosity between Spec Cu and OFHC Cu can be attributed to differences in the ease with which climb occurs or to differences in the number or "potency" of nuclei cannot be clearly established. However, since climb is already difficult in both cases, it seems more reasonable to assume that the differences in porosity are due to the presence of more effective nuclei for vacancy agglomeration in OFHC copper.

The possibility that defects which are found in quenched metals and alloys (i.e., dislocation loops and stacking fault tetrahedra) might actually represent an intermediate step in the formation of porosity observed in diffusion couples recently has been considered.[53] This possibility seems unlikely since defects of this type are formed in the presence of an excess vacancy concentration far greater than that which exists in diffusion couples. It is felt that the magnitude of the excess vacancy concentrations normally developed in diffusion couples is far too small to enable either dislocation loops or stacking fault tetrahedra to nucleate. In addition, collapsed vacancy discs and stacking fault tetrahedra are known to anneal out at temperatures well below those usually employed in diffusion experiments and, therefore, they would not be expected to be stable at the diffusion temperature.

The concentration-penetration curves (see Fig. 14) for OFHC Cu/Ni and Spec Cu/Ni couples do not exactly superimpose. This could possibly be the result of enhanced diffusion through the vapor phase or along pore surfaces. Since the vapor pressure of nickel is lower than that of copper by a factor of 10^5 at the diffusion temperature, pores might, in fact, act as closed circuits for the transport of nickel and open circuits for copper.[44] As

was pointed out by Thomas and Birchenall,[54] if surface and vapor diffusion are fast compared with volume diffusion around a pore, porosity will accelerate diffusion. If surface and vapor transport are slow compared with volume diffusion, diffusion will be inhibited. Translation of the pore produces a greater average displacement of the richer component on the side of the couple toward which the pore is moving, i.e., Cu. Therefore, because of the presence of a greater pore volume in the OFHC Cu/Ni couple, enhanced vapor transport or surface diffusion might possibly have occurred to a greater extent, this could account for the observed differences in the c-x curves.

V. CONCLUSIONS

1. The differences in the nature, distribution and amount of porosity observed in OFHC Cu/Ni and Spec Cu/Ni couples are attributed to differences in the number and/or effectiveness of available nuclei for vacancy condensation.
2. The location of the porous zone and the distribution of pores within this zone is not dependent upon the orientation of individual grains nor upon the availability of grain boundaries in copper/nickel couples.
3. The overal expansion of OFHC Cu/Ni and Spec Cu/Ni couples is accounted for quantitatively by the formation of porosity in the diffusion zone.
4. Approximately 50% of the net vacancy flux goes to form pores in Spec Cu, whereas 80-90% of the vacancies agglomerate as pores in OFHC Cu.
5. It appears that dislocations do not provide very effective sinks for vacancies during diffusion processes in copper/nickel couples.
6. It is estimated that pores will form when vacancies are pumped into any small region of the diffusion zone at the rate of about $10^{15}/cm^3/sec$ in OFHC Cu/Ni and $10^{17}/cm^3/sec$ in Spec Cu/Ni.
7. The relative excess concentration of vacancies in the diffusion zone at the locations where pores initially form is estimated as approximately 0.0003 in OFHC Cu/Ni and 0.02 in Spec Cu/Ni after 720 h of diffusion at 900°C.
8. Aluminum oxide particles or clusters in silver appear to have influenced the normal distribution of porosity in silver-gold diffusion couples, and are, therefore, believed to be acting as favorable sites for vacancy condensation.

APPENDIX

In a binary alloy, e.g., Cu-Ni, the weight percent copper is given by the ratio of the corrected intensity of the characteristic CuK_α radiation emitted by the sample and that obtained from the pure standard. Corrections to the measured X-ray intensities must, in general, be made for:[55-57] a) absorption in the sample and in the standard, b) fluorescence effects, c) back scattering of electrons, d) variations in the specific decelerating power of electrons with atomic number.

The copper-nickel system appears to be nearly ideal since all of the required corections are small. As Poole[56] has shown, both c) and d) are negligible when the atomic numbers of the components are nearly identical, as is the case with copper (Z = 29) and nickel (Z = 28). No fluorescence correction need be applied to the observed CuK_α intensities since neither NiK_α and NiK_β excites the K shell of copper. The absorption correction is also quite small inasmuch as the mass absorption coefficients of copper and nickel for CuK_α and NiK_α are small and of the same order of magnitude.[58] Nevertheless, an absorption correction has been made in accordance with the method proposed by Birks.[39] The magnitude of this correction is less than 1.0% over the entire concentration range and is therefore of the same order as the uncertainty in the measurements themselves. The resulting calibration curve relating relative intensities of CuK_α to atomic percent copper, is shown in Fig. 18.

Since the K shell of nickel is excited by the CuK_β radiation, a fluorescence correction would be necessary when making the analysis with respect to NiK_α. This effect should be small, but might be significant enough to account for the fact that the sum of the relative intensities $I_{Cu}/I(Cu)$ and $I_{Ni}/I(Ni)$ departs from unity by as much as 3% in the intermediate composition ranges.

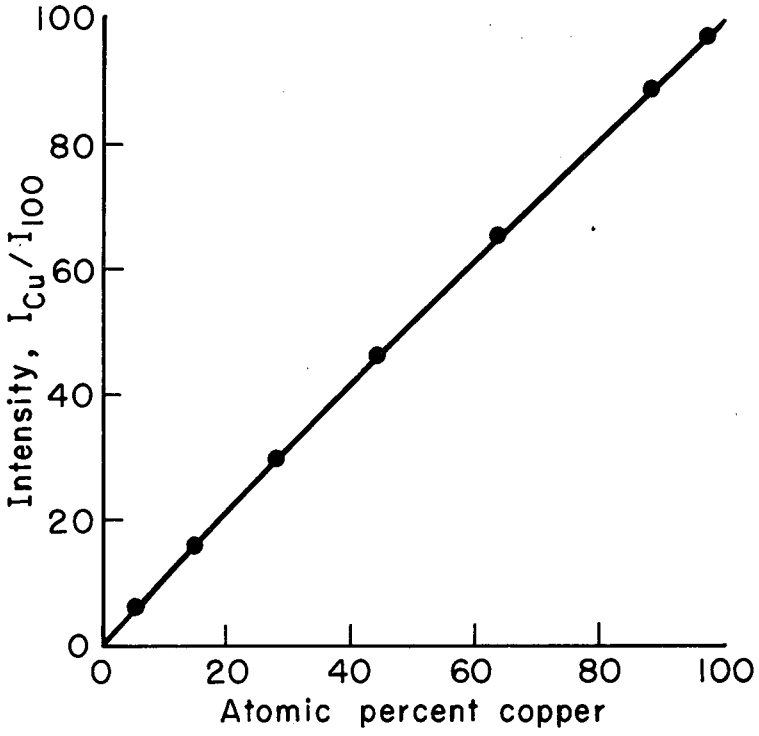

Fig. 18. Calibration curve. Relative Cuk$_\alpha$ x-ray emission intensity vs atomic percent copper in nickel.

ACKNOWLEDGMENT

This investigation was carried out in the Inorganic Materials Research Division, Lawrence Radiation Laboratory of the University of California under the support of the United States Atomic Energy Commission. The author is indebted to Dr. L. Himmel for his guidance, encouragement, and patience throughout the duration of the work. In addition, he is grateful to Professor J. Dorn for the enlightening discussions, to the Metallurgy Department at the Ford Scientific Laboratory in Dearborn, Michigan for the generous use of their electron probe microanalyzer and to Mr. H. Domian for his assistance in the operation of the unit.

REFERENCES

1. A. D. LeClaire, Progress in Metal Physics, 1, 306 (1949); 4, 265 (1953).
2. D. Lazarus, Solid State Physics, 10, 71 (1960).
3. A. D. Smigelskus and E. O. Kirkendall, Trans. AIME, 171, 130 (1947).
4. L. C. Correa da Silva and R. F. Mehl, Trans. AIME, 191, 155 (1951).
5. A. D. LeClaire and R. S. Barnes, Trans. AIME, 191, 1060 (1951).
6. R. S. Barnes, Proc. Phys. Soc. B65, 572 (1952).
7. R. W. Balluffi and B. H. Alexander, J. Appl. Phys. 23, 1237 (1952).
8. H. Bückle and J. Blin, J. Inst. Metals, 80, 385 (1952).
9. W. Seith and A. Kottmann, Angew. Chem. 64, 379 (1952).
10. W. Seith and A. Kottmann, Naturwiss. 39, 40 (1952).
11. Th. Heumann and A. Kottmann, Z. Metallkunde, 44, 139 (1953).
12. R. W. Balluffi and L. L. Seigle, J. Appl. Phys. 25, 607 (1954).
13. R. W. Balluffi, Acta Met. 2, 194 (1954).
14. W. Seith and R. Ludwig, Z. Metallkunde, 45, 401 (1954).
15. R. W. Balluffi and L. L. Seigle, Acta Met. 3, 170 (1955).
16. R. Resnick and R. W. Balluffi, Trans. AIME, 203, 1004 (1955).
17. R. S. Barnes, Rept. Conf. Defects in Crystal Solids, London; J. Inst. Metals, 23, 995 (1956).
18. R. Resnick and L. L. Seigle, Trans. AIME, 209, 87 (1957).
19. Th. Heumann and G. Walther, Z. Metallkunde, 48, 151 (1957).
20. R. Resnick and L. L. Seigle, J. Appl. Phys. 28, 513 (1957).
21. R. S. Barnes and D. J. Mazey, Acta Met., 6, 1 (1958).
22. V. Ruth, Z. Physik. Chem. N. F., 20, 313 (1959).
23. A. Bolk, Acta Met., 9, 632 (1961).
24. F. Rhines and R. F. Mehl, Trans. AIME, 128, 185 (1938).

25. R. W. Balluffi and B. Alexander, J. Appl. Phys., 23, 953, 1407 (1952).

26. V. Y. Doo and R. W. Balluffi, J. Appl. Phys. 30, 325 (1959).

27. J. Bardeen and C. Herring, Imperfections in Nearly Perfect Crystals, p. 261, John Wiley and Sons, New York (1952).

28. F. Seitz, Acta Met. 1, 355 (1953).

29. R. W. Balluffi and L. L. Seigle, Acta Met. 5, 449 (1957).

30. J. A. Brinkman, Acta Met. 3, 140 (1955).

31. L. L. Seigle and R. Resnick, Acta Met., 3, 605 (1955).

32. J. A. Brinkman, Acta Met. 3, 606 (1955).

33. M. F. Ashby and G. L. Smith, Phil. Mag. 5, 298 (1960).

34. L. S. Darken, Trans. Quarterly A.S.M., 54, 599 (1961).

35. F. N. Rhines, Trans. AIME, 137, 246 (1940).

36. F. N. Rhines, W. A. Johnson and W. A. Anderson, Trans. AIME, 147, 205 (1941).

37. P. Rothstein and F. R. Turner, Symposium on Methods of Metallographic Specimen Preparation, A.S.T.M., Special Technical Publication No. 285, 90 (1961).

38. R. S. Barnes, Nature, 166, 1032 (1950).

39. L. S. Birks, J. Appl. Phys., 32, 387 (1961).

40. C. J. Meechan and Guy W. Lehman, J. Appl. Phys., 33, 634 (1962).

41. E. D. Hondros and A. J. W. Moore, Acta Met., 8, 647 (1960).

42. R. King, Thesis, London University (1955).

43. J. Crank, The Mathematics of Diffusion, p. 219, Oxford University Press (1956).

44. R. W. Balluffi, Trans. AIME 197, 726 (1953).

45. C. Matano, Japanese Journal of Physics, 8, 109 (1933).

46. M. Cohen, C. Wagner and J. E. Reynolds, Trans. AIME 197, 1534 (1953); 200, 702 (1954).

47. L. S. Darken, Trans. AIME 175, 184 (1948).

48. A. D. LeClaire, Trans. AIME, 175, 194 (1948).

49. F. Seitz, Trans. AIME, 215, 359 (1959).

50. OFHC Brand Copper Technical Survey, p. 76 (American Metal Climax, Inc., 1961).

51. A. Howie and P. R. Swann, Phil. Mag., 6, 1215 (1961).

52. P. R. Thornton, T. E. Mitchell and P. B. Hirsch, Phil. Mag., 7, 1349 (1962).

53. (Miss) A. G. van Zuilichem and W. G. Burgers, Phil. Mag., 7, 981 (1962).

54. D. E. Thomas and C. E. Birchenall, Trans. AIME, 197, 727 (1953).

55. R. Castaing, Thesis, University of Paris (1951); (ONERA Publ. No. 55).

56. R. Castaing, Advances in Electronics and Electron Physics, XIII, 317 (1960).

57. D. M. Poole and (Miss) P. M. Thomas, J. Inst. Metals, 90, 228 (1962).

58. K. Sagel, Tabellen zur Röntgenspektralanalyse, (Berlin, 1959).

59. V. Ruth, Thesis, Institut für physikalische Chemie, University of Göttingen, Germany, 1961.

60. V. Ruth, Trans. Met. Soc. AIME, 227, 778 (1963).

61. R. O. Simmons and R. W. Balluffi, Phys. Rev. 129, 1533 (1963).

62. R. W. Balluffi, J. S. Koehler and R. O. Simmons, Recovery and Recrystallization of Metals, L. Himmel, ed., Interscience, New York, (1963).

63. H. Kimura, R. Maddin and D. Kuhlmann-Wilsdorf, Acta Met. 7, 145 (1959).

64. J. Lothe, J. Appl. Phys., 31, 1077 (1960).

65. R. M. Thomson and R. W. Balluffi, J. Appl. Phys., 33, 803 (1962).

66. P. B. Hirsch, Phil. Mag., 7, 67 (1962).

67. B. Escaig, Acta Met., 11, 595 (1963).